

Chapter 2

Thermodiffusion Models

Abstract Three approaches to study *thermodiffusion* in binary and multicomponent mixtures are explored in this chapter, viz., the nonequilibrium thermodynamics, algebraic correlations, and artificial neural network. The first method employs the principles of nonequilibrium thermodynamics to explain thermodiffusive separation, by considering the heat and mass fluxes in the mixture as linear functions of forces such as temperature gradient and chemical potential. The second method is based on the observation of relations between the thermodiffusion parameters and parameters such as the mixture composition and pure component/mixture properties. Finally, in artificial neural networks, a data mining of a reasonably large set of experimental data is undertaken and a model is developed that predicts the thermodiffusion data based on the principles of associative thinking. To this end, mathematical functions are integrated in the model to quantify the decision-making process. Expressions corresponding to all three methods are discussed in this chapter.

2.1 Linear Nonequilibrium Thermodynamic Theory

In many irreversible processes, the state variables are functions of space and time. Hence, in studying such systems, it becomes essential to formulate the basic equations in a way so as to refer to quantities at a single point in space. In other words, a local formalism of the fundamental equations is necessary. To this end, a theoretical framework for the macroscopic description of the irreversible processes is provided by the theory of nonequilibrium thermodynamics.

The key aspect of the theory of nonequilibrium thermodynamics is the *entropy* balance for an infinitesimally small volume element. *Entropy* is a thermodynamic property that can be used to determine the energy not available for work in a thermodynamic process. It has a unit of JK^{-1} . The change in entropy in this volume element is due to two reasons, viz.,

1. Entropy flux into the element
2. Entropy production inside the volume element

Thus, a transport equation for the change in entropy would be of the form

$$\frac{ds}{dt} = -\text{div}\mathbf{J}_s + \sigma \quad (2.1)$$

$$\sigma \geq 0. \quad (2.2)$$

In the above equation, s is the entropy per unit mass, σ is the entropy production per unit volume per unit time or simply entropy production strength. Finally, \mathbf{J}_s is the total entropy flux per unit area per unit time less the convective contribution in this flux. It must be noted that in the transport equation (2.1), the second term on the right side is the source term. Further, since entropy can only be created, for an entropy balance, this source term is always positive, as indicated by (2.2).

Now, in order to relate the entropy source to the irreversible processes in the system, a complete set of macroscopic governing equations is generally written for a local volume element to account for the transport of mass, species, momentum, and energy. Using these and the Gibbs thermodynamic relation, one can develop a relation between the rate of change of entropy and other parameters, viz., rate of change of internal energy, rate of change of composition, and rate of change of specific volume. In particular, it is assumed that within the small mass element of interest, an equilibrium state exists, *local*, if one may add, although the entire system in itself might not be in a state of equilibrium. For such a small element, along the center of mass, we can write the Gibbs equation as

$$T \frac{ds}{dt} = \frac{du}{dt} + P \frac{dv}{dt} - \sum_{k=1}^n \mu_k \frac{dc_k}{dt}, \quad (2.3)$$

where u is the specific internal energy, P is the pressure, v is the specific volume and μ_k is the chemical potential.

2.1.1 Phenomenological Equations

As is customary in any set of governing equations, an equation of state is also included for closure. However, despite this, the set of governing equations including the equation for entropy balance and the equation of state cannot be solved with the initial and boundary conditions. This is due to the presence of the irreversible fluxes that are unknown in this set of equations. To address this issue, a set of *phenomenological equations* are also included in this system of equations. These phenomenological equations relate the unknown irreversible fluxes *linearly* with the thermodynamic forces in the entropy strength, and would be called the *linear phenomenological equations*, i.e.,

$$J_i = \sum_k L_{ik} \Phi_k, \quad (2.4)$$

where J_i is a component of the flux in the direction i , L_{ik} are the phenomenological coefficients and Φ_i is the thermodynamic force in the direction i . It must be noted that the entropy production is related to the fluxes and the forces as

$$\sigma = \sum_k J_k \Phi_k. \quad (2.5)$$

In summary, the entire set of partial differential equations consisting of the governing equations, phenomenological equations, and the equations of state is complete, and can be solved using the initial boundary conditions to study the irreversible process.

Extensive details of the theory of nonequilibrium thermodynamics have been presented in the book of de Groot and Mazur [21] and will not be pursued further here. Instead, in the following section, drawing from these principles of linear of nonequilibrium thermodynamics theory, relevant equations pertinent to the derivations of the formalisms for thermodiffusion processes will be discussed.

2.2 Method 1: Thermodiffusion Models Based on LNET Theory

For a n -component mixture at a temperature T and pressure P , if we assume that the only external force acting on the system is gravity (\mathbf{g}), then we can write the entropy production strength as

$$\sigma = -\frac{1}{T^2} \mathbf{J}'_q \cdot \nabla T - \frac{1}{T} \sum_{k=1}^n \mathbf{J}_k \cdot (\nabla T \mu_k - \mathbf{g}), \quad (2.6)$$

where \mathbf{J}_k is the molar diffusion flux relative to the molar average velocity of the k th component. The vector \mathbf{J}'_q is the heat flux due to pure conduction heat flow and is given as

$$\mathbf{J}'_q = \mathbf{J}_q - \sum_{k=1}^n h_k \mathbf{J}_k. \quad (2.7)$$

In the above equation, \mathbf{J}_q is the total heat flux and h_k is the partial specific enthalpy of the k th component. Thus, the total heat flux consists of two parts, viz., heat flux due to pure conduction, denoted by \mathbf{J}'_q , and heat flux due to the diffusion of mass, denoted by the term $\sum_{k=1}^n h_k \mathbf{J}_k$.

Another method of expressing \mathbf{J}'_q is to use the concept of net heat of transport [8, 54]. As per this representation,

$$\mathbf{J}'_q = \sum_{k=1}^n Q_k^* \mathbf{J}_k, \quad (2.8)$$

where Q_k^* is the net heat of transport of the k th component. More specifically, it is the conductive heat flow of the k th component per particle per mole or per kilogram, required to be absorbed by the local region to keep the temperature of the region constant.

Now, keeping in mind that $\sum_k \mathbf{J}_k = 0$, in a n -component system, there are $n - 1$ independent fluxes and so the entropy production strength in (2.6) can be written as

$$\sigma = -\frac{1}{T^2} \mathbf{J}'_q \cdot \nabla T - \frac{1}{T} \sum_{k=1}^{n-1} \mathbf{J}_k \cdot (\nabla T (\mu_k - \mu_n)). \quad (2.9)$$

Further, incorporating (2.8) in the above expression, we get

$$\sigma = -\sum_{k=1}^{n-1} \left[(Q_k^* - Q_n^*) \frac{\nabla T}{T^2} + \frac{\nabla T (\mu_k - \mu_n)}{T} \right] \cdot \mathbf{J}_k. \quad (2.10)$$

At this time, one can write phenomenological equations for the diffusion mass flux in terms of the phenomenological coefficients as

$$\mathbf{J}_i = -\sum_{k=1}^{n-1} L_{ik} \left[(Q_k^* - Q_n^*) \frac{\nabla T}{T} + \nabla T (\mu_k - \mu_n) \right], \quad (2.11)$$

or slightly more explicitly as

$$\mathbf{J}_i = -\sum_{k=1}^{n-1} L_{ik} \left[(Q_k^* - Q_n^*) \frac{\nabla T}{T} + \sum_{j=1}^{n-1} \frac{\partial \mu_k}{\partial x_j} \nabla x_j \right]. \quad (2.12)$$

An additional way of writing the diffusion flux equations is by using the transport coefficients in conjunction with the gradients of temperature, pressure, and concentration. This will yield

$$\mathbf{J} = -\chi (\mathbf{D}_M \nabla \mathbf{x} + \mathbf{D}_T \cdot \nabla T + \mathbf{D}_P \cdot \nabla P), \quad (2.13)$$

where \mathbf{D}_M , \mathbf{D}_T and \mathbf{D}_P represent the molecular diffusion coefficients, thermodiffusion coefficients, and barodiffusion coefficients, respectively, and χ is the mole density. Further, \mathbf{D}_M is a matrix with elements $\mathbf{D}_M = [D_{ij}]$. On the other hand, $\mathbf{D}_T = (\mathcal{D}_T^{(1)}, \mathcal{D}_T^{(2)}, \dots, \mathcal{D}_T^{(n-1)})$, $\mathbf{D}_P = (D_P^{(1)}, D_P^{(2)}, \dots, D_P^{(n-1)})$ and $\nabla \mathbf{x} = (\nabla x_1, \nabla x_2, \dots, \nabla x_{n-1})$ are vectors. In the absence of any pressure gradient, the above equation reduces to

$$\mathbf{J} = -\chi (\mathbf{D}_M \nabla \mathbf{x} + \mathbf{D}_T \cdot \nabla T). \quad (2.14)$$

From (2.12) and (2.14) we can deduce the expression for the thermodiffusion coefficient as

$$\mathcal{D}_T^{(i)} = \frac{\sum_{k=1}^{n-1} (Q_k^* - Q_n^*) L_{ik}}{\chi \times T}. \quad (2.15)$$

2.2.1 The Net Heat of Transport

From (2.15) it is clear that for an accurate estimate of the thermodiffusion coefficient, precise evaluation of Q^* is essential. As mentioned earlier, Q^* is the amount of energy which must be absorbed by the region per mole of a component while diffusing out in order to maintain the constancy in the temperature and pressure of the mixture. To this end, we can represent it in terms of the energy needed to detach a molecule from its neighbors and the energy given out when a molecule fills the hole. In this, we can use the viscous energy as an approximation of the energy needed to detach a molecule. For a multicomponent mixture, an expression for Q^* has been proposed by Firoozabadi and coworkers [19] as

$$Q_i^* = \frac{U_i}{\tau_i} + \left(\sum_{j=1}^n x_j U_j / \tau_j \right) \frac{V_j}{\sum_{k=1}^n x_k V_k}, \quad (2.16)$$

where τ_i is the ratio of the cohesive and viscous energy, of component i . U_i and V_i are the partial molar internal energy and partial molar volume, respectively.

2.2.2 Equation of State

An equation of state is used to determine the state parameters such as density, pressure, fugacity, and enthalpy. Depending upon the type of mixture being studied, different equations of state have been developed in the literature. For instance, the Peng–Robinson (*PR*) equation of state [43] is more suited to the hydrocarbon mixtures than water alcohol mixtures. For the latter type of mixtures, the Perturbed Chain Statistical Associating Fluid Theory (*PC-SAFT*) equation of state [22, 23] is more accurate. While there are other choices available for an equation of state (e.g., Cubic Plus Association equation of state), the user must extensively evaluate them with respect to experimental data before selecting them for a particular type of mixture. Two equations of state are now discussed below to highlight the difference between their formulations.

2.2.2.1 Peng–Robinson Equation of State

In the Peng–Robinson equation of state [43], the parameters are expressed in terms of the critical properties and the acentric factor. It is applicable to liquid as well as gas phase, and is fairly accurate near the critical point. In particular, it has good prediction capabilities for the compressibility factor and liquid density.

Density: To calculate density, the following equation is used:

$$\rho = \frac{P}{ZRT}M, \quad (2.17)$$

where Z is the unknown compressibility factor, R is the universal gas constant, and M is the mixture molar mass. The pressure, P , is the second unknown in this equation.

Pressure: Pressure is calculated using the relation

$$P = \frac{RT}{V-b} - \frac{a}{V(V+b) + b(V-b)}. \quad (2.18)$$

where V is the molar volume, a and b are the attraction and co-volume parameters, respectively. Both a and b are functions of temperature, and their formulations will be discussed shortly.

Compressibility factor: To calculate the compressibility factor, (2.18) is first rearranged as

$$\left(P + \frac{a}{V(V+b) + b(V-b)} \right) (V-b) = RT. \quad (2.19)$$

Now, comparing (2.17) and (2.19), we can write a cubic polynomial in Z as

$$Z^3 - (1-B)Z^2 + (A-3B^2-2B)Z - (AB-B^2-B^3) = 0. \quad (2.20)$$

In the above equation,

$$A = \frac{aP}{(RT)^2}, \quad (2.21a)$$

$$B = \frac{bP}{RT}. \quad (2.21b)$$

It must be noted that the number of roots of this polynomial is governed by the number of phases in the system.

If one applies (2.19) at critical temperature (T_c) and critical pressure (P_c), then we get

$$a|_{T=T_c} = 0.45724 \frac{(RT_c)^2}{P_c}, \quad (2.22)$$

$$b|_{T=T_c} = 0.0778 \frac{RT_c}{P_c}, \quad (2.23)$$

$$Z_c = 0.3070. \quad (2.24)$$

While $b = b|_{T=T_c}$ at other temperatures, a is calculated as

$$a(T) = a(T_c)\theta(T_r, \omega). \quad (2.25)$$

Thus, a is scaled via a dimensionless function of reduced temperature (T_r) and acentric factor (ω). The precise equation for θ is

$$\theta = \left[1 + \beta \left(1 - \sqrt{T/T_c} \right) \right]^2, \quad (2.26)$$

where, depending upon the range of ω

$$\beta = 0.37464 + 1.54226\omega - 0.26992\omega^2; 0 < \omega < 0.5, \quad (2.27)$$

$$\beta = 0.3796 + 1.485\omega - 0.1644\omega^2 + 0.01667\omega^3; 0.5 < \omega < 2.0. \quad (2.28)$$

It must be noted that this dimensionless function (θ) evaluates to 1 at $T = T_c$.

Fugacity coefficient: The fugacity of the component in the mixture is calculated using the relationship

$$\begin{aligned} \ln \frac{\phi_k}{x_k P} &= \frac{b_k}{\sum_i x_i b_i} (Z - 1) - \ln(Z - B) - \frac{A}{2\sqrt{2}B} \\ &\times \left(\frac{2 \sum_j X_j a_{ik}}{\sum_i \sum_j x_i x_j a_{ij}} - \frac{b_k}{\sum_i x_i b_i} \right) \ln \left(\frac{Z + 2.414B}{Z - 0.414B} \right). \end{aligned} \quad (2.29)$$

In the above equation, a_{ij} is related to an empirically determined binary interaction coefficient between the components i and j , viz., δ_{ij} , and is given as

$$a_{ij} = (1 - \delta_{ij})\sqrt{a_i a_j}. \quad (2.30)$$

Enthalpy: Enthalpy is calculated as

$$H = H_{\text{ideal}} + RT(Z - 1) + \frac{T \frac{da}{dT} - a}{2\sqrt{2}b} \ln \left(\frac{Z + 2.414B}{Z - 0.414B} \right), \quad (2.31)$$

where H_{ideal} is the enthalpy of the ideal gas at the same temperature and pressure conditions.

Volume translated Peng–Robinson equation of state: The *volume translated* Peng–Robinson (v -PR) equation of state is a slight modification of the PR equation of state to improve the volumetric predictions. In this, the following shift parameter, ϵ , is introduced [34]

$$\epsilon = 1 - d/M^e. \quad (2.32)$$

In the above equation, d and e are constants that depend upon the mixture. For example, for n-alkanes, $d = 2.258$ and $e = 0.1823$. With this shift parameter, the corrected molar volume is

$$V_{\text{corrected}} = V_{\text{PR}} - \varepsilon x_i b_i. \quad (2.33)$$

As a result of this small modification, the v - PR equation of state predicts the equilibrium properties of the hydrocarbon mixtures quite accurately.

2.2.2.2 Perturbed Chain Statistical Associating Fluid Theory Equation of State

In Perturbed chain statistical associating fluid theory equation of state, proposed by Gross and Sadowski [22, 23], once again, the density is computed as

$$\rho = \frac{P}{ZRT}M. \quad (2.34)$$

In this expression, unlike PR equation of state, the compressibility factor is calculated using the relation

$$Z = 1 + \eta \left(\frac{\partial \tilde{a}^{\text{res}}}{\partial \eta} \right)_{T, c_i}, \quad (2.35)$$

where \tilde{a}^{res} is the residual Helmholtz free energy and η is the packing fraction.

The residual Helmholtz free energy, \tilde{a}^{res} , that is used to compute the other necessary mixture properties, is the key factor in PC - $SAFT$ equation of state. It is represented as the sum of three contributing factors, viz., the hard chain (\tilde{a}^{hc}), dispersion (\tilde{a}^{disp}), and association (\tilde{a}^{assoc}). The hard chain contribution is computed as

$$\tilde{a}^{\text{hc}} = \bar{m} \tilde{a}^{\text{hs}} - \sum_i c_i (m_i - 1) \ln g_{ii}^{\text{hs}}(\sigma_{ii}), \quad (2.36)$$

where \bar{m} is the mean segment number in the system, m_i is the number of segments per chain of the i th component, and σ_{ii} is the segment diameter. Additionally, in the above equation, the hard sphere fluid's Helmholtz free energy (\tilde{a}^{hs}), and the radial distribution function (g_{ij}^{hs}) are given as

$$\tilde{a}^{\text{hs}} = \frac{1}{\gamma_0} \left[\frac{3\gamma_1 \gamma_2}{(1 - \gamma_3)} + \frac{\gamma_2^3}{\gamma_3(1 - \gamma_3)^2} + \left(\frac{\gamma_2^3}{\gamma_3^2} - \gamma_0 \right) \ln(1 - \gamma_3) \right], \quad (2.37)$$

$$g_{ij}^{\text{hs}} = \frac{1}{(1 - \gamma_3)} + \left(\frac{d_i d_j}{d_i + d_j} \right) \frac{3\gamma_2}{(1 - \gamma_3)^2} + \left(\frac{d_i d_j}{d_i + d_j} \right)^2 \frac{2\gamma_2^2}{(1 - \gamma_3)^3}, \quad (2.38)$$

where γ_k represents

$$\gamma_k = \rho \pi / 6 \sum_i c_i m_i d_i^k. \quad (2.39)$$

In this relation, the temperature-dependent segment diameter, d_i , of the i th component is given in terms of the depth of the potential pair (ε_i) by

$$d_i = \sigma_i \left[1 - 0.12 \exp \left(-3 \frac{\varepsilon_i}{kT} \right) \right]. \quad (2.40)$$

The dispersion contribution to the Helmholtz free energy is

$$\tilde{a}^{\text{disp}} = -2\pi\rho I_1(\eta, \bar{m}) \overline{m^2 \varepsilon \sigma^3} - \pi\rho \bar{m} C_1 I_2(\eta, \bar{m}) \overline{m^2 \varepsilon^2 \sigma^3}, \quad (2.41)$$

where three abbreviations have been used, viz.

$$C_1 = \left(1 + \bar{m} \frac{8\eta - 2\eta^2}{(1 - \eta)^4} + (1 - \bar{m}) \frac{20\eta - 27\eta^2 + 12\eta^3 - 2\eta^4}{(1 - \eta)^2(2 - \eta)^2} \right), \quad (2.42a)$$

$$\overline{m^2 \varepsilon \sigma^3} = \sum_i \sum_j c_i c_j m_i m_j \left(\frac{\varepsilon_{ij}}{kT} \right) \sigma_{ij}^3, \quad (2.42b)$$

$$\overline{m^2 \varepsilon^2 \sigma^3} = \sum_i \sum_j c_i c_j m_i m_j \left(\frac{\varepsilon_{ij}}{kT} \right)^2 \sigma_{ij}^3. \quad (2.42c)$$

In the above equations, σ_{ij} and ε_{ij} are determined as

$$\sigma_{ij} = 0.5(\sigma_i + \sigma_j). \quad (2.43)$$

$$\varepsilon_{ij} = \sqrt{\varepsilon_i \varepsilon_j} (1 - k_{ij}), \quad (2.44)$$

k_{ij} being the binary interaction parameter. In (2.41), the integrals of the perturbation theory, I_1 and I_2 , are approximated via the following expressions

$$I_1(\eta, \bar{m}) = \sum_{i=0}^6 a_i(\bar{m}) \eta^i, \quad (2.45)$$

$$I_2(\eta, \bar{m}) = \sum_{i=0}^6 b_i(\bar{m}) \eta^i. \quad (2.46)$$

The coefficients a_i and b_i in these expressions depend upon the chain length and are given as

$$a_i(\bar{m}) = a_{0,i} + a_{1,i} \frac{\bar{m} - 1}{\bar{m}} + a_{2,i} \frac{\bar{m} - 1}{\bar{m}} \frac{\bar{m} - 2}{\bar{m}}, \quad (2.47)$$

$$b_i(\bar{m}) = b_{0,i} + b_{1,i} \frac{\bar{m} - 1}{\bar{m}} + b_{2,i} \frac{\bar{m} - 1}{\bar{m}} \frac{\bar{m} - 2}{\bar{m}}, \quad (2.48)$$

where $a_{k,i}$ and $b_{k,i}$ are model constants.

Finally, the association contribution, \tilde{a}^{assoc} , is given by

$$\tilde{a}^{\text{assoc}} = \sum_i c_i \sum_{A_i} (\ln X_{A_i} - 0.5 X_{A_i} + 0.5 M_i), \quad (2.49)$$

where M_i is the number of associating sites on the molecule of type i and X_{A_i} is the fraction of A sites that do not form associating bonds with other active sites. Further, X_{A_i} is a solution of the following system of equations:

$$X_{A_i} = \frac{1}{1 + \rho \sum_j c_j \sum_{B_j} X_{B_j} \Delta^{A_i B_j}}, \quad (2.50)$$

where B_j indicates the summation over all the sites and $\Delta^{A_i B_j}$ is a measure of the association strength between site A on molecule i and site B on molecule j . Now, if sites A and B are on the molecules of the same type, then

$$\Delta^{A_i B_j} = \sigma^3 g_H(d_i) \kappa^{A_i B_j} \left[\exp \left(\frac{\epsilon^{A_i B_j}}{k_B T} \right) - 1 \right], \quad (2.51)$$

where $\kappa^{A_i B_j}$ is the association volume and $\epsilon^{A_i B_j}$ is the association energy. On the other hand, if sites A and B are on molecules of different type

$$\Delta^{A_i B_j} = \sqrt{\Delta^{A_i B_i} \Delta^{A_j B_j}}. \quad (2.52)$$

Using the above relations, quantities such as density, pressure, fugacity, enthalpy, and entropy can be determined as derivatives of the residual Helmholtz energy. The computation of these quantities are done as follows:

Density: In order to compute the density at a given system pressure, an iterated approach is followed in which the reduced density (η) is adjusted to match the calculated pressure with the system pressure. Once a value for η is determined, the number density of molecules, ρ , is estimated as

$$\rho = 6/\pi\eta \left(\sum_i c_i m_i d_i \right)^{-1}. \quad (2.53)$$

The molar density $\hat{\rho}$ is then calculated as

$$\hat{\rho} = \frac{\rho}{6.022 \times 10^{23}} \left(10^{10} \frac{\text{\AA}^3}{\text{m}} \right) \left(10^{-3} \frac{\text{kmol}}{\text{mol}} \right). \quad (2.54)$$

Pressure: From the residual Helmholtz free energy, the compressibility factor can be determined as

$$Z = 1 + \eta \left(\frac{\partial \tilde{a}^{\text{res}}}{\partial \eta} \right)_{T, c_i}. \quad (2.55)$$

The pressure is then calculated in the units of Pa as

$$P = Z k T \rho \left(10^{10} \frac{\text{\AA}^3}{\text{m}} \right)^3. \quad (2.56)$$

Fugacity coefficient: The residual chemical potential, μ_k^{res} , is obtained from \tilde{a}^{res} as

$$\frac{\mu_k^{\text{res}}(T, v)}{kT} = \tilde{a}^{\text{res}} + (Z - 1) + \left(\frac{\partial \tilde{a}^{\text{res}}}{\partial c_k} \right)_{T, v, c_{j \neq k}} - \sum_{j=1}^N \left[c_j \left(\frac{\partial \tilde{a}^{\text{res}}}{\partial c_j} \right)_{T, v, c_{i \neq j}} \right]. \quad (2.57)$$

The fugacity coefficient, ϕ_k , is then obtained from the chemical potential as

$$\ln \phi_k(T, v) = \frac{\mu_k^{\text{res}}(T, v)}{kT} - \ln Z. \quad (2.58)$$

Enthalpy and entropy: From the derivative of the residual Helmholtz free energy with respect to temperature, the molar enthalpy, \hat{h}^{res} , is given by the relation

$$\hat{h}^{\text{res}} = RT \left[-T \left(\frac{\partial \tilde{a}^{\text{res}}}{\partial T} \right)_{\rho, c_i} + (Z - 1) \right]. \quad (2.59)$$

The residual entropy at a given pressure and temperature condition is

$$\hat{s}^{\text{res}}(P, T) = -RT \left[\left(\frac{\partial \tilde{a}^{\text{res}}}{\partial T} \right)_{\rho, c_i} + \frac{\tilde{a}^{\text{res}}}{T} \right] + R \ln(Z). \quad (2.60)$$

Finally, from the above two equation, the Gibbs free energy, $\hat{g}^{\text{res}}(P, T)$, is defined as

$$\hat{g}^{\text{res}} = \hat{h}^{\text{res}} - T \hat{s}^{\text{res}}(P, T). \quad (2.61)$$

2.2.3 Binary Liquid Mixtures

A thermodiffusion theory for a multicomponent mixture has been outlined in Sect. 2.2. However, most of the experimental research is conducted on two or more lately on the three component systems. This is primarily because of the complexity of the inter-particle interactions that is not well understood even in such simple systems. Consequently, numerous models have been proposed over time for binary mixtures. Most of these models differ in the way the net heat of transport has been modeled. Additionally, some of the models also incorporate the effects of additional forces that contribute to the separation behavior in the non-isothermal mixtures.

A detailed description of the formulation and derivation of every model in the literature is beyond the scope of this book. Instead, in the ensuing paragraphs, we present an overview of a subset of them, in chronological order, giving adequate references for the reader to pursue them in detail.

2.2.3.1 1955—Dougherty and Drickamer—Model 1

As per this model [10], based on the principles of nonequilibrium thermodynamics, the flux equation for the first component in a binary system, for instance, can be written as

$$J_1 = -\chi D_m \left[\nabla x_1 - \frac{\alpha_T x_1}{x_2} T \nabla T \right]. \quad (2.62)$$

At steady state, the fluxes J_1 and J_2 vanish. Combining this condition with (2.12) for a binary mixture, and noting from the Gibbs–Duhem relation at constant pressure and temperature that

$$\sum_i x_i d\mu_i = 0, \quad (2.63)$$

the thermodiffusion factor, α_T , for a binary system can be written as

$$\alpha_T = \frac{Q_2^* - Q_1^*}{x_1 \frac{\partial \mu_1}{\partial x_1}}. \quad (2.64)$$

Now, in their model, Dougherty and Drickamer [10] related the net heat of transport to the energy needed to create a hole (W_H) and the energy needed to occupy a hole (W_L), respectively. Their model also accounted for the different sizes and shapes of the molecules by considering the different fractions of the two molecules that create and occupy a hole. More precisely,

$$Q_1^* = W_{H1} - \psi_1 W_L \text{ and} \quad (2.65a)$$

$$Q_2^* = W_{H2} - \psi_2 W_L, \quad (2.65b)$$

where

$$\psi_i = \frac{V_i}{x_1 V_1 + x_2 V_2}, \quad (2.66a)$$

$$W_L = x_1 W_{H1} + x_2 W_{H2} \text{ and} \quad (2.66b)$$

$$W_{Hi} = -\frac{1}{\tau_i} (U_i - U_{ig}). \quad (2.66c)$$

In the above equation, τ is the ratio of the energy of vaporization of the liquid and the activation energy of the viscous flow, U_i is the partial molar energy of the i th component, and U_{ig} is the energy of the ideal gas at the corresponding temperature and pressure.

2.2.3.2 1955—Dougherty and Drickamer—Model 2

In this model, the authors proposed a slightly different expression for α_T as [11]

$$\alpha_T = \frac{M_1 Q_2^* - M_2 Q_1^*}{(M_1 x_1 + M_2 x_2) x_1 \frac{\partial \mu_1}{\partial x_1}}. \quad (2.67)$$

Unlike the previous model where the center of mass of the system is assumed stationary, the above expression avoids this hidden assumption. Now, expressing the net heats of transport in terms of W_{Hi} and W_L , α_T is calculated as

$$\alpha_T = \frac{M_2 V_1 + M_1 V_2}{(M_1 x_1 + M_2 x_2) x_1 \frac{\partial \mu_1}{\partial x_1}} \left(\frac{W_{H2}}{V_2} - \frac{W_{H1}}{V_1} \right). \quad (2.68)$$

It must be noted that the convention in the Drickamer models is that if $\alpha_T > 0$ for component-1, then it enriches near the hot side.

2.2.3.3 1956—Tichacek, Kmak, and Drickamer

By discussing the thermodiffusion process in a center-of-volume frame of reference, the authors proposed an expression for α_T as [54]

$$\alpha_T = \frac{V_1 V_2}{(V_1 x_1 + V_2 x_2) x_1 \frac{\partial \mu_1}{\partial x_1}} \left(\frac{M_2 Q_2^*}{V_2} - \frac{M_1 Q_1^*}{V_1} \right). \quad (2.69)$$

2.2.3.4 1969—Haase

While Haase [26] studied the barodiffusion process in isothermal gas mixtures subjected to pressure gradients, he proposed an expression for thermodiffusion in binary electrolyte mixtures, by analogy, as

$$\alpha_T = \frac{M_1 (H_2 - H_2^{(0)}) - M_2 (H_1 - H_1^{(0)})}{(M_1 x_1 + M_2 x_2) x_2 \frac{\partial \mu_2}{\partial x_2}} + \frac{RT}{x_2 \frac{\partial \mu_2}{\partial x_2}} \alpha_0, \quad (2.70)$$

where H is the partial molar enthalpy and α_0 is the thermodiffusion factor for the ideal gas mixture at the corresponding temperature. In the above equation, the first term on the right side is the thermodiffusion factor of the mixture with respect to the ideal gas phase that is indicated by the superscript (0), and the second term is the contribution due to the thermodiffusion in an ideal gas state.

2.2.3.5 1986—Guy

In a barycentric frame of reference, Guy [25] proposed the following expression for thermodiffusion factor in electrolyte solutions:

$$\alpha_T = \frac{M_2 (h_2^{xs} - h_1^{xs})}{x_2 \frac{\partial \mu_2}{\partial x_2}}, \quad (2.71)$$

where h_i^{xs} is the partial excess enthalpy of the i th component in the mixture.

2.2.3.6 1989—Kempers

Following an initial model [35] based on the principles of statistical nonequilibrium thermodynamics, that is similar to the Haase model, in 2001, Kempers [36] proposed revised expressions for thermodiffusion factor in multicomponent systems. In particular, two expressions of his work that correspond to the *center-of-volume* and *center-of-mass* frames of reference, applicable to binary systems, are as follows:

Center of volume frame of reference

$$\alpha_T = \left(\frac{V_1 V_2}{V_1 x_1 + V_2 x_2} \right) \frac{\frac{(H_2 - H_2^{(0)})}{V_2} - \frac{(H_1 - H_1^{(0)})}{V_1}}{x_1 \frac{\partial \mu_1}{\partial x_1}} + \frac{RT}{x_1 \frac{\partial \mu_1}{\partial x_1}} \alpha_{T0}. \quad (2.72)$$

Center of mass frame of reference

$$\alpha_T = \left(\frac{M_1 M_2}{M_1 x_1 + M_2 x_2} \right) \frac{\frac{(H_2 - H_2^{(0)})}{M_2} - \frac{(H_1 - H_1^{(0)})}{M_1}}{x_1 \frac{\partial \mu_1}{\partial x_1}} + \frac{RT}{x_1 \frac{\partial \mu_1}{\partial x_1}} \alpha_{T0}. \quad (2.73)$$

In the above equations, α_{T0} is the thermodiffusion factor of the mixture at the corresponding temperature in the ideal gas state.

2.2.3.7 1998—Shukla and Firoozabadi

Coupling the model of Drickamer with the volume translated Peng–Robinson equation of state, Shukla and Firoozabadi proposed a model for α_T in binary liquid mixtures as [50]

$$\alpha_T = \frac{\frac{U_1}{\tau_1} - \frac{U_2}{\tau_2}}{x_1 \frac{\partial \mu_1}{\partial x_1}} + \frac{(V_2 - V_1) \left(x_1 \frac{U_1}{\tau_1} + x_2 \frac{U_2}{\tau_2} \right)}{(x_1 V_1 + x_2 V_2) x_1 \frac{\partial \mu_1}{\partial x_1}}. \quad (2.74)$$

It is worth noting that the sign convention in this expression is that when $\alpha_T > 0$ for component-1, it enriches near the cold side.

2.2.3.8 2008—Artola, Rousseau, and Galliero

Following the propositions of Prigogine [44], Artola et al. [1] proposed the following expression based on the principles of nonequilibrium thermodynamics:

$$\alpha_T = \frac{\Delta G_2 - \Delta G_1}{RT} + \frac{M_2 - M_1}{M_1 + M_2} \frac{\Delta G_1 + \Delta G_2}{RT}. \quad (2.75)$$

In the above equation, ΔG_i is the activation-free enthalpy of the i th component and is obtained as

$$D_i = D_{i0} \exp(-\Delta G_i/RT). \quad (2.76)$$

In this equation, D_i and D_{i0} are the self diffusion coefficients at current temperature T and reference temperature T_0 , respectively.

2.2.3.9 Other Expressions Based on Activation Energy of Viscous Flow

Several other models have evolved in the study of thermodiffusion, which are particularly influenced by the work of Tichacek et al. [54], modeling the net heat of transport via an activation energy of viscous flow (E^{vis}). While a universal model for thermodiffusion is still lacking in the literature, as outlined below, one can find different expressions for α_T for different types of mixtures, viz., nonassociating liquids [12], associating liquids [13], polymers [17], and DNA solutions [18].

Nonassociating liquid mixtures, e.g., hydrocarbon liquid mixtures [12]:

$$\alpha_T = \frac{E_1^{\text{vis}} - E_2^{\text{vis}}}{x_1 \frac{\partial \mu_1}{\partial x_1}}, \quad (2.77)$$

$$\alpha_T = \frac{M_2 E_1^{\text{vis}} - M_1 E_2^{\text{vis}}}{(M_1 x_1 + M_2 x_2) x_1 \frac{\partial \mu_1}{\partial x_1}}, \quad (2.78)$$

$$\alpha_T = \frac{V_2 E_1^{\text{vis}} - V_1 E_2^{\text{vis}}}{(V_1 x_1 + V_2 x_2) x_1 \frac{\partial \mu_1}{\partial x_1}}. \quad (2.79)$$

In addition to the above expressions, one can also use a weighted combination of (2.78) and (2.79) as a measure of α_T .

Associating liquid mixtures, e.g., water–alcohol mixtures [13]:

$$\alpha_T = \frac{M_2 (E_1^{\text{vis}} - E_{\text{mix}}^{\text{vis}}) - M_1 (E_2^{\text{vis}} - E_{\text{mix}}^{\text{vis}})}{(M_1 x_1 + M_2 x_2) x_1 \frac{\partial \mu_1}{\partial x_1}}, \quad (2.80)$$

$$\alpha_T = \frac{V_2 (E_1^{\text{vis}} - E_{\text{mix}}^{\text{vis}}) - V_1 (E_2^{\text{vis}} - E_{\text{mix}}^{\text{vis}})}{(V_1 x_1 + V_2 x_2) x_1 \frac{\partial \mu_1}{\partial x_1}}. \quad (2.81)$$

While these two equations are not particularly good in their predictions, an equation that performs somewhat better is given as

$$\alpha_T = - \frac{E_1^{\text{vis}} - E_2^{\text{vis}}}{x_1 \frac{\partial \mu_1}{\partial x_1}} \frac{\partial \ln(\eta_{\text{mix}}/\eta_0)}{\partial x_1}, \quad (2.82)$$

where η_0 is a reference viscosity, e.g., viscosity of water (1 cP at room temperature). In this last expression, by including a term containing the derivative of the natural logarithm of viscosity with respect to the composition, there is an attempt to account for the nonlinear relation between the mixture viscosity and composition, which is often observed in associating mixtures. Thus, by including this term, the sign change in the thermodiffusion factor has been forced at the maxima or minima on the $\ln(\eta)$ versus x_1 graph.

Dilute polymer and DNA solutions [18]:

$$\alpha_T = \frac{E_M^{\text{vis}} a \ln\left(\frac{2M_P}{M_M}\right) - E_S^{\text{vis}}}{RT}, \quad (2.83)$$

where M_P and M_M are the molecular weights of the polymer and monomer, respectively. a is a polymer-solvent characteristic parameter that varies between 0.5 and 0.8. E_S^{vis} and E_M^{vis} are the activation energy of viscous flow of the solvent and the monomer, respectively.

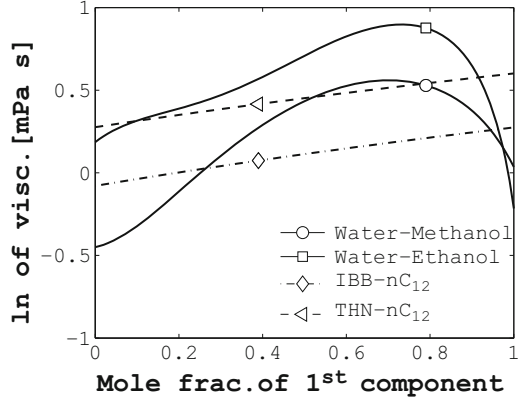
2.2.3.10 A Note on the Activation Energy of Viscous Flow

As mentioned at the beginning of Sect. 2.2.3.9, in (2.77)–(2.83) the net heat of transport Q_i^* for the i th component has been calculated by correlating it with activation energy of viscous flow. In this, by applying Eyring's rate theory [20], viscosity of a liquid can be related to the activation energy of the viscous flow. In particular, in the vicinity of the temperature of interest, if we plot the natural logarithm of the experimental data of viscosity or its product with the molar volume against $1/RT$, the graph exhibits a straight line with a slope corresponding to the activation energy of viscous flow. More precisely

$$E_i^{\text{vis}} \approx \frac{\partial \ln \eta}{\partial (1/T)}. \quad (2.84)$$

This calculation of activation energy of viscous flow is applicable for nonassociating mixtures like liquid hydrocarbons.

Fig. 2.1 Natural logarithm of viscosity plotted against the mole fraction of the first component. The trends are for the experimental data obtained from [51] for associating (water–alcohol) mixtures and from [3] for nonassociating (hydrocarbon) mixtures. IBB is isobutylbenzene, nC₁₂ is n-dodecane, and THN is tetralin



For the activation energy of viscous flow for the mixture ($E_{\text{mix}}^{\text{vis}}$) in (2.80)–(2.82), the above correlation cannot be used. This is because in associating mixtures like water–alcohol, for instance, there is a nonlinear relationship between $\ln \eta$ and $1/RT$. This is clearly evident in Fig. 2.1 where the natural logarithm of viscosity for two representative water–alcohol mixtures are plotted alongside the viscosity data of two hydrocarbon mixtures. The reason behind the nonlinear trend in these associating mixtures is that with the change in the concentration of the liquid, the interactions between the molecules and the structure of the mixtures change. One way to account for these changes is to simply multiply the expressions of α_T by a correction term, $E_{\text{mix}}^{\text{vis}}$, which is prescribed as [13]

$$E_{\text{mix}}^{\text{vis}} \approx \frac{\partial \ln(\eta_{\text{mix}}/\eta_0)}{\partial x}. \quad (2.85)$$

This gives us the corrected α_T as in (2.82). Note that the above equation is also incorporated in (2.80) and (2.81).

The calculation of the activation energy of viscous flow in the polymer solutions is even more complicated. This is because polymers are in solid state at room temperature although they are soluble in certain liquids, resulting in a liquid mixture. Now, with most of the thermodiffusion experiments on polymer solutions being performed at room temperatures, viscosity data of pure polymer at room temperature is unavailable.

On the other hand, what is known of polymers is that in dilute polymer solutions, small sections of these long chain molecules called *beads* or *segments* move independent of each other. It must be noted that this is valid only for a very low concentration of the polymer in the mixture. So, in this case, we can use the activation energy of the viscous flow of the monomers that represent the moving segments, instead of the activation energy of the polymer. This is something that can be calculated since the monomers are usually in liquid state even at

room temperatures. Now, for the activation energy, viscosity data are needed. One correlation that can be used is the Mark–Houwink equation [30],

$$\eta = KM_p^a, \quad (2.86)$$

where K is a constant dependent on the polymer-solvent system. Using the above expression, we can obtain the activation energy of viscous flow of the polymer as

$$E_p^{\text{vis}} = \frac{d \ln(V\eta)}{d(1/RT)} \ln \left(\frac{M_p}{M_B} \right)^a, \quad (2.87)$$

where M_B is the molecular weight of the moving segment of the polymer and the other notations have the usual meaning, as defined before.

2.2.3.11 Other Theoretical Formulations

While the nonequilibrium thermodynamic approaches using the net heats of transport have been a fairly popular approach to study thermodiffusion and formulate theoretical equations for this phenomenon in different mixtures, there are other theories for the thermodiffusive separation.

A hydrodynamic approach: In this approach to study thermodiffusion, one can express the thermodiffusional driving force as a combination of equilibrium and nonequilibrium terms [41]. The equilibrium term can be attributed to the temperature gradient of the partial pressure. Further, by applying the solvation theory to the inter-particle interactions, one can write

$$S_T = \frac{1}{n_1 \kappa_B T} \left(\frac{\partial p_1}{\partial T} \right)_{p, c_1 \rightarrow 0}, \quad (2.88)$$

where n_1 , p_1 , and c_1 are the number of moles, partial pressure, and the concentration of the first component, i.e., the solute.

By theoretically defining the partial pressure, Morozov [41] deduced two useful expressions for the Soret coefficient as

$$S_T = \frac{1}{n_2 T} \left[\frac{\partial (n_2 T Z_{12})}{\partial T} \right]_p, \quad (2.89)$$

$$S_T = \frac{1}{n_2 T} \left[\frac{\partial (n_2 T [Z_{12} - Z_2])}{\partial T} \right]_p. \quad (2.90)$$

In the above equations, n_2 is the number of moles of solvent, Z_{12} is the compressibility factor of the first component in the solvent, and Z_2 is the compressibility factor of the solvent.

Statistical thermodynamics approach: By considering thermodiffusion on the basis of statistical thermodynamics and force balance, one can express the thermodiffusion coefficient in terms of the pair-interaction potential between the colloidal spheres [9]. More precisely,

$$D_T = D_0 \beta \frac{\partial \Pi}{\partial T}, \quad (2.91)$$

where D_0 is the Einstein's translational diffusion coefficient, $\beta = 1/\kappa_B T$, κ_B being the Boltzmann constant, and Π is the osmotic pressure. This osmotic pressure is a function of the colloid number density, temperature, and the chemical potential of the pure solvent with which the suspension is in osmotic equilibrium, and is given as

$$\Pi = \rho \kappa_B T - \frac{2\pi}{3} \rho^2 \int_0^\infty r^3 g^{\text{eq}} \frac{df}{dr} dr, \quad (2.92)$$

where r is the distance between the two colloidal spheres and f is the pair-interaction potential of mean force. g^{eq} is the equilibrium pair-correlation function which for low colloidal concentrations is given as

$$g^{\text{eq}} = \exp(-\beta f). \quad (2.93)$$

2.2.4 Ternary Liquid Mixtures

Recent advances in experimental techniques has resulted in experimental investigations on thermodiffusion in ternary liquid mixtures. Theoretical framework for studying ternary mixtures has been around for much longer though. Of course, the general multicomponent formulation of Sect. 2.2 with $n = 3$ will give an expression for the ternary mixture as well. Nevertheless, there are some formulations for the thermodiffusion coefficients in ternary mixtures in the literature. Here we present two sets of expressions for the thermodiffusion coefficients in ternary mixtures, one for nonassociating liquids and the other for associating liquids, as outlined by Eslamian and Saghir [14].

The starting point of the derivation for both associating and nonassociating liquid mixtures is the molar flux of the i th component in a n -component mixture that can be written as

$$\mathbf{J}_i = - \sum_{k=1}^n L_{ik} \left[Q_k^* \frac{\nabla T}{T} + \sum_{j=1}^{n-1} \frac{\partial \mu_k}{\partial x_j} \nabla x_j \right], \quad i = 1, \dots, n. \quad (2.94)$$

At steady state, for a ternary mixture ($n = 3$), the flux of each component is zero, i.e., $\mathbf{J}_1 = \mathbf{J}_2 = \mathbf{J}_3 = 0$. In other words, we have

$$\frac{\partial \mu_1}{\partial x_1} \nabla x_1 + \frac{\partial \mu_1}{\partial x_2} \nabla x_2 = -Q_1^* \frac{\nabla T}{T}, \quad (2.95a)$$

$$\frac{\partial \mu_2}{\partial x_1} \nabla x_1 + \frac{\partial \mu_2}{\partial x_2} \nabla x_2 = -Q_2^* \frac{\nabla T}{T}, \quad (2.95b)$$

$$\frac{\partial \mu_3}{\partial x_1} \nabla x_1 + \frac{\partial \mu_3}{\partial x_2} \nabla x_2 = -Q_3^* \frac{\nabla T}{T}. \quad (2.95c)$$

In writing the above system of equations, it is noted that the phenomenological coefficients are nonzero and can therefore be eliminated. Further, since the fluxes of only two components are independent, we can eliminate the third equation in the above system using the Gibbs–Duhem relation at constant temperature and pressure conditions, and writing $\frac{\partial \mu_3}{\partial x_1}$ and $\frac{\partial \mu_3}{\partial x_2}$ in terms of the chemical potentials and mole fractions of the first two components. This modifies the above system of equations as

$$B_{11} \nabla x_1 + B_{12} \nabla x_2 = -(Q_1^* - Q_3^*) \frac{\nabla T}{T}, \quad (2.96a)$$

$$B_{21} \nabla x_1 + B_{22} \nabla x_2 = -(Q_2^* - Q_3^*) \frac{\nabla T}{T}, \quad (2.96b)$$

where B_{ij} are elements of the matrix \mathbf{B} , and are given as

$$B_{11} = \left[\frac{\partial \mu_1}{\partial x_1} \left(1 + \frac{x_1}{x_3} \right) + \frac{\partial \mu_2}{\partial x_1} \left(\frac{x_2}{x_3} \right) \right], \quad (2.97a)$$

$$B_{12} = \left[\frac{\partial \mu_1}{\partial x_2} \left(1 + \frac{x_1}{x_3} \right) + \frac{\partial \mu_2}{\partial x_2} \left(\frac{x_2}{x_3} \right) \right], \quad (2.97b)$$

$$B_{21} = \left[\frac{\partial \mu_2}{\partial x_1} \left(1 + \frac{x_2}{x_3} \right) + \frac{\partial \mu_1}{\partial x_1} \left(\frac{x_1}{x_3} \right) \right], \quad (2.97c)$$

$$B_{22} = \left[\frac{\partial \mu_2}{\partial x_2} \left(1 + \frac{x_2}{x_3} \right) + \frac{\partial \mu_1}{\partial x_2} \left(\frac{x_1}{x_3} \right) \right]. \quad (2.97d)$$

To calculate the derivatives of the chemical potential one can employ an appropriate equation of state to first calculate the fugacity and its derivative for the i th component. Subsequently, these values can be used to calculate $\frac{\partial \mu_i}{\partial x_j}$ using the relation

$$\frac{\partial \mu_i}{\partial x_j} = \frac{RT}{f_i} \frac{\partial f_i}{\partial x_j}. \quad (2.98)$$

As noted previously, one can write the flux equations using the transport coefficients as

$$\mathbf{J}_1 = -\chi (D_{11} \nabla x_1 + D_{12} \nabla x_2 + \mathcal{D}_T^1 \nabla T), \quad (2.99a)$$

$$\mathbf{J}_2 = -\chi (D_{21} \nabla x_1 + D_{22} \nabla x_2 + \mathcal{D}_T^2 \nabla T), \quad (2.99b)$$

where D_{ij} are the components of the 2×2 matrix for molecular diffusion, viz., \mathbf{D} . Also, it must be noted that for the above system of equations, $\sum_i \mathcal{D}_T^i = 0$. Once again, at steady state, in the absence of any flux, the left side of the above system can be set to zero and we can compare the above equations to (2.96) to obtain the thermodiffusion coefficients as

$$\mathcal{D}_T^1 = \frac{d(Q_1^* - Q_3^*) - b(Q_2^* - Q_3^*)}{T(ad - bc)}, \quad (2.100a)$$

$$\mathcal{D}_T^2 = \frac{-c(Q_1^* - Q_3^*) + a(Q_2^* - Q_3^*)}{T(ad - bc)}, \quad (2.100b)$$

where

$$a = \frac{B_{11}D_{22} - B_{12}D_{21}}{|\mathbf{D}|}, \quad (2.101a)$$

$$b = \frac{-B_{11}D_{12} + B_{12}D_{11}}{|\mathbf{D}|}, \quad (2.101b)$$

$$c = \frac{B_{21}D_{22} - B_{22}D_{21}}{|\mathbf{D}|}, \quad (2.101c)$$

$$d = \frac{-B_{21}D_{12} + B_{22}D_{11}}{|\mathbf{D}|}. \quad (2.101d)$$

Nonassociating mixtures: For the nonassociating mixtures like liquid hydrocarbons, in (2.100) we can use the activation energy of viscous flow as a measure of the net heat of transport, i.e.,

$$Q_i^* = E_i^{\text{vis}}. \quad (2.102)$$

This will get us the thermodiffusion coefficients for the ternary mixture as¹

$$\mathcal{D}_T^1 = \frac{d(E_1^{\text{vis}} - E_3^{\text{vis}}) - b(E_2^{\text{vis}} - E_3^{\text{vis}})}{T(ad - bc)}, \quad (2.103a)$$

$$\mathcal{D}_T^2 = \frac{-c(E_1^{\text{vis}} - E_3^{\text{vis}}) + a(E_2^{\text{vis}} - E_3^{\text{vis}})}{T(ad - bc)}. \quad (2.103b)$$

Associating mixtures: As in the case of the expressions for the binary associating mixtures, the contributions due to the nonlinear relationship between the natural logarithm of viscosity and the composition of the mixture must be taken into account even in the ternary formulations. This can be done by multiplying each $(E_i^{\text{vis}} - E_j^{\text{vis}})$

¹We would like to caution the readers that in [15] these equations were validated using an incorrect experimental data. The authors inadvertently used a wrong sign of the experimental data in the validation of these expressions with respect to the ternary hydrocarbon mixtures of n-dodecane-isobutylbenzene-tetralin.

term in (2.103) by a factor corresponding to the rate of change of the viscosity of a binary mixture of components i and j with respect to the mole fraction of component i . As a result, (2.103) gets modified for a ternary mixture of associating liquids as [16]

$$\mathcal{D}_T^1 = \frac{d(E_1^{\text{vis}} - E_3^{\text{vis}}) \left(\frac{-\partial \ln(\eta_{13}/\eta_0)}{\partial x_1} \right) - b(E_2^{\text{vis}} - E_3^{\text{vis}}) \left(\frac{-\partial \ln(\eta_{23}/\eta_0)}{\partial x_2} \right)}{T(ad - bc)}, \quad (2.104a)$$

$$\mathcal{D}_T^2 = \frac{-c(E_1^{\text{vis}} - E_3^{\text{vis}}) \left(\frac{-\partial \ln(\eta_{13}/\eta_0)}{\partial x_1} \right) + a(E_2^{\text{vis}} - E_3^{\text{vis}}) \left(\frac{-\partial \ln(\eta_{23}/\eta_0)}{\partial x_2} \right)}{T(ad - bc)}. \quad (2.104b)$$

In the above equation, the coefficients a, b, c , and d are as described in (2.101). η_{ij} is the viscosity of the binary mixture of component i and j .

2.3 Method 2: Simple Algebraic Expressions to Quantify Thermodiffusion

In the previous section, a detailed formalism of the thermodynamic approaches to study thermodiffusion in multicomponent mixtures has been presented. The numerous expressions presented, especially the ones requiring extensive thermodynamic data, need to be coupled to an appropriate equation of state to obtain estimates of quantities such as enthalpy, fugacity (to calculate chemical potential), and compressibility factor (for density calculation). On the other hand, following years of research on specific types of mixtures, simpler algebraic equations have been developed which can give a fairly accurate quantitative estimate of the thermodiffusion process. These are discussed in the ensuing paragraphs.

2.3.1 Liquid Hydrocarbon Mixtures

Several expressions are found in the analysis of the experimental data of different nonassociating mixtures, hydrocarbons in particular. One type of analysis procedure is to choose a binary mixture of two components and study the thermodiffusion in this mixture at different composition, or different temperatures. Such analyses cast light on the composition and temperature effects in the thermodiffusion process. Another type of analysis is to keep one component fixed and change the second component. This study, for instance, can yield information on the effect of the relative molecular weights of the participating components.

Several empirical correlations have been proposed after studying numerous binary systems. The correlations presented are for the Soret coefficient or for the thermodiffusion coefficient. A very often postulated relation for the Soret coefficient is

$$S_T \propto T^{-2}. \quad (2.105)$$

However, this power law is not true for all mixtures.

One correlation for a binary hydrocarbon mixture suggests that the Soret coefficient can be expressed in terms of composition- and temperature-dependent functions as [56]

$$S_T(x, T) = \theta(x)\phi(T) + S_T^i, \quad (2.106)$$

where $\theta(x)$ is a composition-dependent function, $\phi(T)$ is a temperature-dependent amplitude factor, and S_T^i is a constant offset that is independent of composition as well as temperature. These composition- and temperature-dependent functions are polynomials that are written as

$$\theta(x) = a_0 + a_1x^2 + a_3x^3 + \dots, \quad (2.107a)$$

$$\phi(T) = 1 + b_1(T - T_0) + b_2(T - T_0)^2 + \dots. \quad (2.107b)$$

In the above equations, a_i and b_i are constants that are empirically determined and T_0 is a reference temperature. Further, the degree of these polynomials would depend on the type of binary mixture studied, and is also determined empirically based on some experimental data about the mixture of interest.

Another such closely related algebraic formulation is [29]

$$S_T(x, T) = \theta(x)\phi(T) + c \frac{M_2 - M_1}{M_2 M_1}, \quad (2.108)$$

where c is a constant with a unit of K^{-1} . In addition to the composition and the operating temperature, this relation also incorporates the difference between the two participating molecules via the molecular weight term.

In a binary hydrocarbon mixture of two very similar molecules, if one investigates the isotopic effects by introducing varying degrees of deuteration, for instance, we can present the Soret coefficient as a sum of two contributions. The first contribution is due to the difference between the mass and the moment of inertia of the two components. This contribution is independent of the composition of the mixture and is attributed to the isotopic effect. The second term arises from the *chemical* contribution and is a function of composition. Thus, the Soret coefficient can be represented as [7]

$$S_T = S_T^c + (a\delta M + b\delta I), \quad (2.109)$$

where a (K^{-1}) and b (K^{-1}) are empirically determined coefficients. S_T^c (K^{-1}) is also empirically determined by regression analysis of the experimental data and has a form

$$S_T^c = (m_1x + m_2)m_0, \quad (2.110)$$

where m_0 (K^{-1}), m_1 and m_2 are constants, and x is the mole fraction of the first component. δM and δI correspond to the effects of mass and moment of inertia, respectively, and are given as

$$\delta M = \frac{M_2 - M_1}{M_1 + M_2}, \quad (2.111a)$$

$$\delta I = \frac{I_2 - I_1}{I_1 + I_2}, \quad (2.111b)$$

where I_i is the moment of inertia of the i th component.

It must be noted that (2.109) only valid over a very narrow range of molecular masses and moments of inertia. A slight modification to this equation, making it accurate for a much wider range, has been proposed by Wittko and Köhler [55] as

$$S_T = S_T^c + (a\Delta M + b\Delta I), \quad (2.112)$$

where

$$\Delta M = M_2 - M_1, \quad (2.113a)$$

$$\Delta I = I_2 - I_1. \quad (2.113b)$$

By expressing the Soret coefficient as a function of the *absolute* difference instead of the *relative* difference of molecular weights and the moments of inertia, the range of equation has been extended.

In equimolar binary n-alkane mixtures, a quantitative estimate of the thermodiffusion coefficient can be obtained via a simple algebraic formulation that is essentially a polynomial in relative molecular weight. This is based on the fact that a simple quadratic relation exists between the thermodiffusion coefficient and the relative molecular weight, as shown in Fig. 2.2. This correlation is expressed as [2]

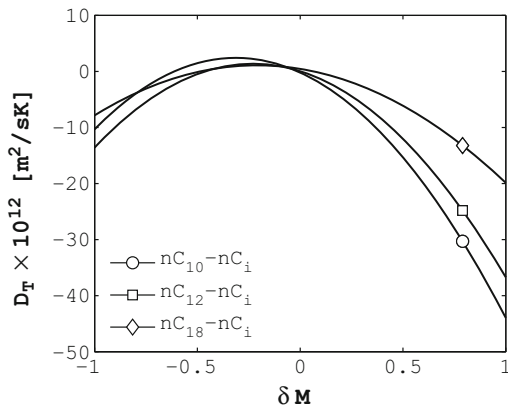
$$D_T = D_{T0} \delta M (1 + \lambda \delta M), \quad (2.114)$$

where D_{T0} is a reference thermodiffusion coefficient that is different for different n-alkane series and λ is a mixture-specific constant.

Algebraic correlations for the thermodiffusion coefficients can also be written in terms of the mixture thermodynamic properties such as dynamic viscosity and thermal expansion coefficients. For the equimolar binary n-alkane series considered in Fig. 2.2, viz., $n\text{C}_{10}-n\text{C}_i$, $n\text{C}_{12}-n\text{C}_i$, and $n\text{C}_{18}-n\text{C}_i$, Blanco et al. [2] have noted that there is a linear relation between the absolute molecular weight difference and Ω , i.e., $\Delta M \propto \Omega$, where Ω is defined as

$$\Omega = \frac{c_2 c_r D_T \eta}{\beta}, \quad (2.115)$$

Fig. 2.2 A quadratic trend between the thermodiffusion coefficients reported in [2] and the relative molecular weight in (2.111a) for equimolar binary n-alkane mixtures. nC₁₀ is n-decane, nC₁₂ is n-dodecane, and nC₁₈ is n-octadecane. Figure modified from [2]



where the subscripts r and 2 are for the reference species and the second species, respectively, and β is the thermal expansion coefficient. A linear relationship between ΔM and Ω implies that we can write the thermodiffusion coefficient for the n-alkane mixtures as

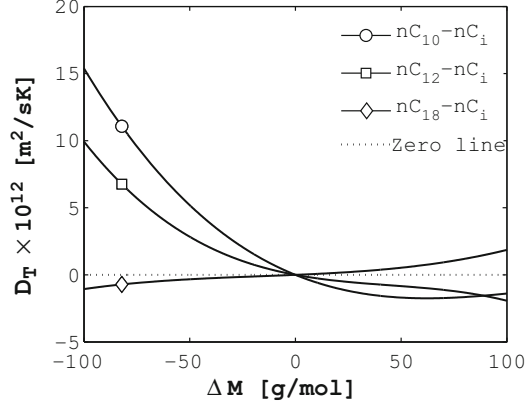
$$D_T = K(M_r - M_2) \frac{\beta}{\eta c_r c_2}, \quad (2.116)$$

where K (m s^{-2}) is the proportionality constant.

To understand the formulation of (2.116), two points are worth noting:

1. The extent of the separation due to thermodiffusion in a binary mixture is governed by the amount of *similarity* between the molecules. The larger the similarity, the smaller the separation process and vice versa. A measure of the similarity between the molecules is the difference between their molecular weights (defined by ΔM in (2.113a)). This concept of similarity between the molecules is shown in Fig. 2.3 where $\Delta M = M_2 - M_r$ is plotted against D_T . We can see that as the difference between the molecular weights increases, the thermodiffusion coefficient increases.
2. A closer look at the figure reveals that D_T increases rapidly as the molecular weight of the second species (M_2) becomes much smaller than the reference species ($\Delta M \ll 0$). However, if the molecular weight of the second species is much larger than the molecular weight of the reference species ($\Delta M \gg 0$), the value of D_T is not very large. This is despite a large dissimilarity between the molecules. This is because when $\Delta M \gg 0$, the viscosity of the mixture increases, leading to decreased mobility of the species. At this point, if we recall the activation energy of viscous flow concept used to quantify thermodiffusion, it is noted that the energy needed to set the molecules in motion is very high for highly viscous fluids. So, in a highly simplistic algebraic model, one can use the viscosity of the mixture account for the mobility of the species in the mixture.

Fig. 2.3 The relation between the difference of the molecular weights of the two components in the binary mixture and the thermodiffusion coefficient of several binary n-alkane mixtures that are reported in [2]



In (2.116), the similarity between the molecules is reflected in the term $(M_r - M_2)$ and the mobility is represented quantitatively by the inverse of viscosity. Of course, for equimolar mixtures,

$$c_r c_2 = \frac{M_r M_2}{(M_r + M_2)^2}, \quad (2.117)$$

which transforms (2.116) to

$$D_T = K(M_r - M_2)(M_r + M_2)^2 \frac{\beta}{\eta M_r M_2}. \quad (2.118)$$

Two issues with (2.114) and (2.116) are:

1. The constants in these equations are mixture specific. Hence, before employing these expressions, prior experimental data are needed to calculate these constants.
2. These equations are only valid for equimolar mixtures.

The first problem can be fixed by extending (2.114) for non-equimolar mixtures by introducing a correction term. More precisely, by including a linear or quadratic term to account for the effect of the mole fraction of the species, we can write two equations for the thermodiffusion coefficient in binary n-alkane mixtures as

$$D_T = D_{T0} \delta M (1 + \lambda_1 \delta M + \lambda_2 (x_r - x_2)), \quad (2.119a)$$

$$D_T = D_{T0} \delta M (1 + \lambda_1 \delta M + \lambda_2 (x_r - x_2) + \lambda_3 (x_r - x_2)^2), \quad (2.119b)$$

where x_r and x_2 are the mole fraction of the reference species and the second species, respectively. λ_i are series specific dimensionless constants. As before, D_{T0} is a reference thermodiffusion coefficient that is different for different binary n-alkane series. Note that for an equimolar case, these expressions reduce to (2.114).

Despite the aforementioned formulation in (2.119), making it valid for a much wider composition, we still need experimental data to determine the various

Table 2.1 Values of D_{T0} and λ_i in (2.121) and (2.122)

Equation #	$D_{T0} \times 10^{17}$ [m ² s ⁻¹ K ⁻¹]	λ_1	λ_2	$\lambda_3 \times 10^4$ [mol g ⁻¹]
(2.121)	4.905	-0.114	-0.122	-3.27
(2.122)	1.213	-0.094	-1.053	-1.86

These constants are the same for any binary n-alkane mixture of any composition

constants in this equation. This drawback is unlikely to be fixed in this enhanced formulation that presents thermodiffusion coefficients solely in terms of the molecular weights and composition. On the other hand, by pursuing (2.116) that takes into account the mixture properties, one can extend/modify it to be valid for non-equimolar mixtures and also avoid the need for experimental data to determine any constants. To this end, an empirical equation proposed by Madariaga et al. [39] is

$$D_T = K_0(x_r)(M_r - M_2) \frac{\beta}{\eta c_r c_2}, \quad (2.120)$$

where $K_0(x_r) = (5.34x_r - 7x_r^2 + 1.65x_r^3) \times 10^{-14} \text{ m s}^{-2}$.²

Another formulation that is also valid for a wide range of n-alkane series of any composition and which does not need any prior data to determine the model constants is

$$D_T = D_{T0} \left(x_r + \lambda_1 \Delta x + \lambda_2 (\Delta x)^2 + \lambda_3 \Delta M^{\text{mix}} \right) \frac{\beta \Delta M^{\text{mix}}}{\eta c_r c_2}, \quad (2.121)$$

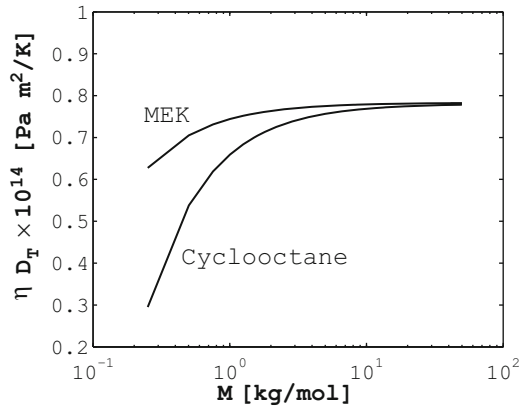
where $\Delta x = x_r - x_2$ and $\Delta M^{\text{mix}} = M_r - M_{\text{mix}}$, M_{mix} being the molecular weight of the mixture. A slight variation of the above equation is

$$D_T = D_{T0} \left(x_r + \lambda_1 \Delta x + \lambda_2 (\Delta x)^2 + \lambda_3 \Delta M \right) \frac{\beta \Delta M}{\eta c_r c_2}. \quad (2.122)$$

All three formulations ((2.120), (2.121), and (2.122)) are very accurate in predicting the thermodiffusion coefficients in any binary n-alkane mixture. The constants D_{T0} and λ_i in the latter two expressions are summarized in Table 2.1. Again, it must be emphasized that these constants in (2.121) and (2.122) do not change with the n-alkane series.

²In the original reference [39], this exponent has been incorrectly typed as -11 m s^{-2} .

Fig. 2.4 The trend of ηD_T against M for PS in two different solvents, viz., cyclooctane and MEK. The trends are based on the experimental data reported in [53]. Figure modified from [53]



2.3.2 Liquid Polymer Mixtures

Unlike alkanes, theoretical considerations for polymers reveal that viscosity of the solvent plays a more dominant role in the thermodiffusion of polymer solutions. For instance, if one looks at the thermodiffusion in solutions of polystyrene (PS) in toluene [46], it is found that for a molar mass in the range of 5 – 4,000 kg mol⁻¹, D_T is independent of the molar mass for almost any concentration. In fact, the thermodiffusion coefficient is purely dictated by the microscopic local viscosity, η_{eff} , and one can write a very simple expression for D_T and S_T in such mixtures as

$$D_T = \frac{\Delta_T}{\eta_{\text{eff}}}, \quad (2.123a)$$

$$S_T = \frac{6\pi R_h^a \Delta_T}{(1 - \phi)^2 \kappa_B T}, \quad (2.123b)$$

where Δ_T (Pa m² K⁻¹) is a constant that depends upon the polymer. R_h^a and ϕ are the apparent hydrodynamic radius of the polymer and volume fraction of the polymer, respectively. Further, in a very dilute solution, $\eta_{\text{eff}} = \eta_s$, the viscosity of the solvent.

In case of oligomers and short polymer chains, D_T increases with the molecular weight of the polymer and eventually reaches a steady state value for very large M . This trend is seen in Fig. 2.4, where the variation of the product ηD_T with the molecular weight is plotted for the solution of PS in two solvents, viz., cyclooctane and methyl ethyl ketone (MEK). In fact, an analysis of PS in various solvents reveals that the thermodiffusion coefficient can be represented as [53]

$$D_T = \frac{\Delta_T}{\eta} - \frac{a}{M^\alpha}, \quad (2.124)$$

where η is the viscosity of the solvent and a (kg m² s⁻¹ K⁻¹ mol⁻¹) is a amplitude factor that depends upon the solution. From the above equation it is clear that for

small values of M , there is an impact of M on D_T . However, for large values, i.e., when the Kuhn segments are more than 1 kg mol^{-1} , the second term becomes irrelevant and the equation looks like (2.123a). More precisely, it is seen that the thermodiffusion coefficient can simply be written as

$$D_T \approx 0.6 \times 10^{-14} \times \eta^{-1}. \quad (2.125)$$

Two other correlations are applicable for the dilute polymer solutions. The first one is proposed by Khazanovich [37] and the other one is by Semenov and Schimpf [48]. According to Khazanovich [37], the thermodiffusion coefficient can be written as

$$D_T = \frac{D_b E_{A,s}}{RT^2}, \quad (2.126)$$

where D_b is the self diffusion coefficient of the bead, R is the gas constant, and $E_{A,s}$ is the activation energy. D_b can be calculated using the hydrodynamic radius, R_b , and the solvent viscosity, η_s , as

$$D_b = \frac{\kappa_B T}{6\pi\eta_s R_b}. \quad (2.127)$$

The activation energy can be expressed in terms of the viscosity data of the solvent as

$$E_{A,s} = -RT^2 \frac{d \ln \eta_s}{dT}. \quad (2.128)$$

Since (2.126) makes use of an activation energy principle, one can argue that this expression is more appropriate in the thermodynamic models considered in Sect. 2.1. Nevertheless, due to the fact that this is a much simpler expression requiring only the viscosity data for calculating the derivative in (2.128), we present it in this section.

According to the correlation presented by Semenov and Shimpf [48], for a diminishing concentration of the polymer in a solution, the thermodiffusion coefficient can be estimated as

$$D_T = \frac{8\beta_s \sqrt{A_p A_s} r_m^2}{27v_s \eta_s} \left(1 - \sqrt{\frac{A_s}{A_p}} \right), \quad (2.129)$$

where β_s is the cubic thermal expansion coefficient of the solvent and r_m is the radius of the monomer. A_p and A_s are the Hamaker constants of the monomer and the solvent, respectively. v_s is the volume occupied by each solvent molecule and is calculated as

$$v_s = \frac{M_s}{\rho_s N_a}, \quad (2.130)$$

where N_a is the Avogadro number.

There is also a simple equation proposed by Brenner [5] following a kinematic analysis which presents the thermodiffusion coefficient as

$$D_T = \lambda \beta_s D_s^s, \quad (2.131)$$

where λ is a non-ideality factor that is of $O(1)$ and is equal to one for ideal gas mixtures, and D_s^s is the self-diffusion coefficient of the solvent.

Finally, if one considers the temperature effects on the Soret effect, then it is found that the Soret coefficient varies with the mixture temperature via a simple correlation as

$$S_T = S_T^\infty \left[1 - \exp\left(\frac{T^* - T}{T_0}\right) \right], \quad (2.132)$$

where T^* is the temperature at which the temperature switching occurs and T_0 is some reference temperature in Kelvin. It must be noted that since the numerator of the exponent is a difference between two temperatures, the choice of Celsius or Kelvin should not matter.

2.3.3 Colloidal Mixtures

Thermodiffusion is studied as thermophoresis in colloidal mixtures. The objective in these studies is to determine the separation behavior of the suspended particles in the presence of a temperature gradient in the mixture. Currently, a good physical understanding of thermophoresis is still considerably poor and the direction of separation is also quite unpredictable. While the dispersed particles mostly move to the cold side, there is some experimental evidence showing an opposite result as well. Nevertheless, our current understanding of thermophoresis has produced some simple correlations for the process.

Temperature effects on thermophoresis in colloidal solutions can still be represented by (2.132). In fact, several macromolecular and colloidal systems, including mixtures of proteins and polypeptides, follow this equation. The effect of the three parameters, viz., S_T^∞ , T^* and T_0 , on the evolution of this equation is illustrated in Figs. 2.5–2.7. As seen in Fig. 2.5, the amplitude factor, S_T^∞ , dictates the pace at which the Soret coefficient changes with temperature. Small values of S_T^∞ implies a relatively smaller value of dS_T/dT , and also a lower final steady state value of S_T .

T^* has an effect of shifting the null point in the curve. More precisely, a large value of T^* implies a larger temperature at which a change in the sign of S_T occurs. Nevertheless, in view of the fact that S_T^∞ is constant in these curves, all three lines in Fig. 2.6 converge to the same horizontal asymptote of $S_T^\infty = 0.01 \text{ K}^{-1}$.

Finally, the contribution of the reference temperature, T_0 , is similar to the impact of S_T^∞ , i.e., it somewhat controls the pace at which the Soret coefficient changes with temperature. At smaller values of T_0 , the value of dS_T/dT is large and S_T reaches the final steady state value of S_T^∞ at a much earlier operating temperature.

Fig. 2.5 The effect of S_T^∞ on the evolution of (2.132). In all three curves shown in the figure $T^* = 15^\circ\text{C}$ and $T_0 = 20\text{ K}$

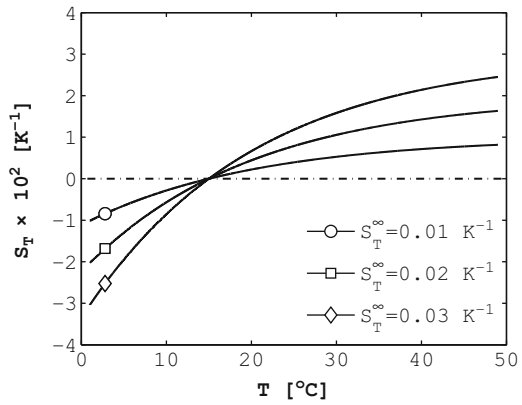


Fig. 2.6 The effect of T^* on the evolution of (2.132). In all three curves shown in the figure $S_T^\infty = 0.01\text{ K}^{-1}$ and $T_0 = 20\text{ K}$

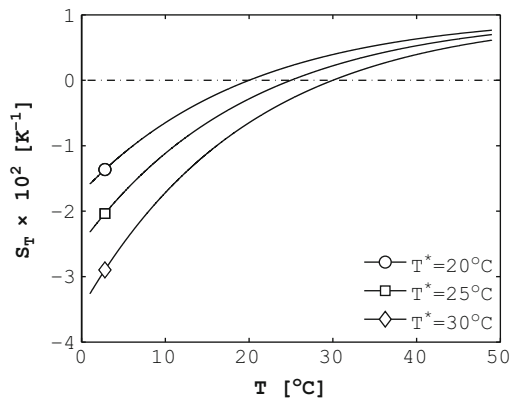


Fig. 2.7 The effect of T_0 on the evolution of (2.132). In all three curves shown in the figure $S_T^\infty = 0.01\text{ K}^{-1}$ and $T^* = 15\text{ K}$

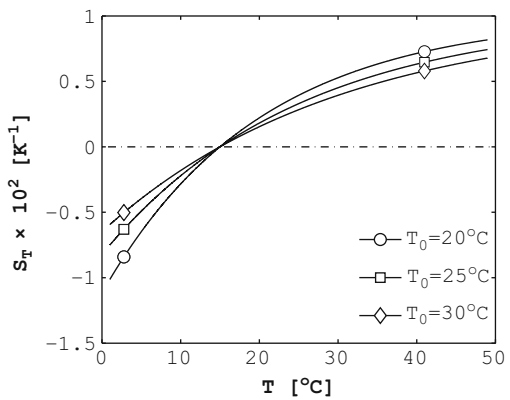
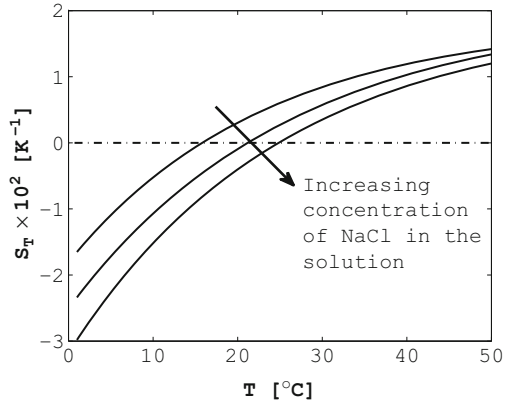


Fig. 2.8 The effect of temperature on the Soret coefficient of lysozyme solutions with varying amounts of NaCl. These trends are on the experimental data reported by Iacopini and Piazza [32]. Figure modified from [32]



The three parameters just discussed can vary due to a change in the ionic strength of the solution that can be controlled by adding salt, NaCl for instance, in the solution. This is illustrated in Fig. 2.8 where (2.132) is plotted for the lysozyme solutions with different concentration of NaCl as investigated by Iacopini and Piazza [32]

One way to interpret thermophoresis is to look at it as a consequence of the drift of particles due to the unbalanced interfacial stresses in the immediate neighborhood of the particle surface. These unbalanced stresses arise due to the temperature inhomogeneity in the mixture. A quantitative consideration of this results in a microscopic hydrodynamic model [33] that presents the Soret coefficient in the colloidal system as

$$S_T = \frac{4\pi r}{\kappa_B T} \frac{\partial(l\gamma)}{\partial T}, \quad (2.133)$$

where r is the particle radius, l is the microscopic length scale that depends upon the range of the interactions between the particle and the solvent, and γ is the particle-solvent interfacial tension.

Unlike the Soret coefficient, the thermodiffusion coefficient varies linearly for many systems including polypeptides, sodium polystyrene sulfonate (NaPSS), polystyrene latex particles, and sodium dodecyl sulfate (SDS)- β -dodecyl-maltoside micellar (DM) solutions [33]. In such solutions, the thermodiffusion coefficient is simply written as

$$D_T = A(T^* - T), \quad (2.134)$$

where A ($\text{m}^2 \text{s}^{-1} \text{K}^{-2}$) is an amplitude factor that depends upon the type of the system investigated.

Thus, in summary, it can be said that numerous thermodiffusion/thermophoresis investigations have identified several empirical correlations that are prescribed either exclusively for a particular system or for a class of liquid mixtures. Although not complete, with little effort in determining the constants and other easily accessible parameters, these correlations can be conveniently employed to study

a variety systems. A primary use of these correlations would be in quickly planning new experiments. In any case, with availability of new experimental data these correlation must be verified and if needed upgraded/corrected.

2.4 Method 3: Neurocomputing Models to Study Thermodiffusion

2.4.1 What are Neural Networks?

Artificial Neural Networks (ANN) or simply *neural networks* (NN) are an attempt to combine the principles of associative approaches and mathematical modeling to develop a *engineering system* that can emulate the human brain. The primary application of such a system would be in studying difficult engineering problems that lack accurate mathematical modeling. Needless to say, before attempting to outline the theoretical framework of such a computational tool, it is pertinent to first introduce some basic neurobiology to understand how the human brain works.

Human brain consists of nearly 100 billion nerve cells that are called *neurons*. A highly simplified example of the functioning of the neurons and the human brain in general is depicted in Fig. 2.9. Essentially, neurons communicate via electrical pulses that are generated via small voltage spikes of the cell walls. The information passes through the *axon* and reaches the other neurons via the *synapses*. Upon receiving these signals, the information is processed and if a sufficient threshold is reached then the recipient neuron will generate a voltage impulse in response. Once again, this is transmitted to the other neurons via the axon. This flow of information/signal is indicated by the arrows in Fig. 2.9.

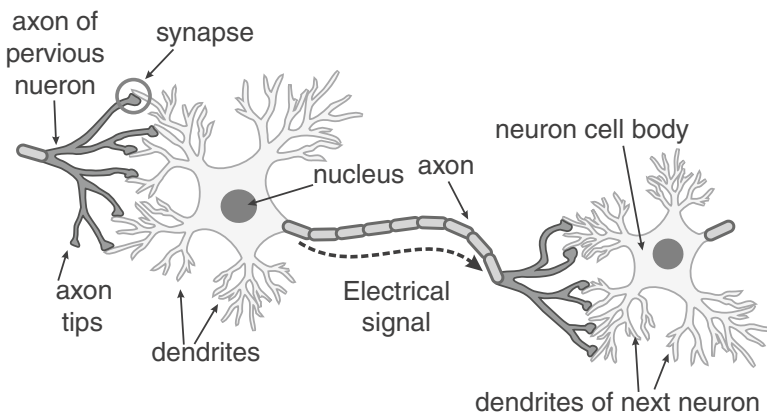


Fig. 2.9 Functioning of a neuron in a simplified format

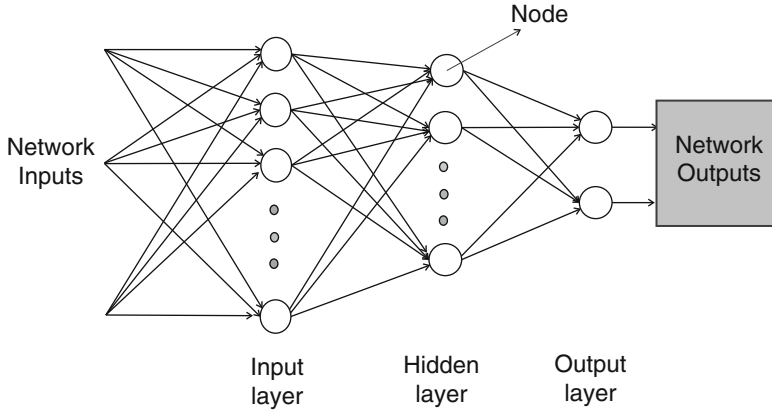


Fig. 2.10 Schematic of an artificial neural network where several layers of nodes are connected

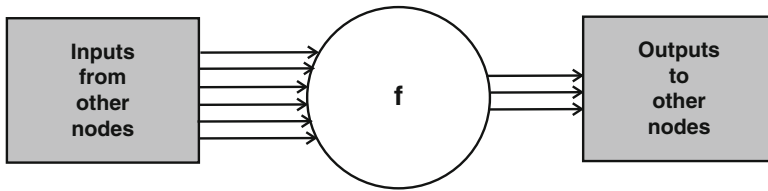


Fig. 2.11 The functionality of a node in an artificial neural network

In solving difficult engineering problems where the response or the output of a system depends upon complex interactions between several parameters that are either known or unknown, this neurobiological principle can be employed to develop what is known as an *Artificial Neural Network*. A schematic of ANN is shown in Fig. 2.10. Thus, analogous to the neurons, we can employ *nodes* that receive inputs from other nodes, evaluate a response function that takes all of these inputs, and calculate an output. A weighted fraction of the output is then passed to the other nodes. A design of a node is depicted in Fig. 2.11. Thus, a more structured definition of an artificial neural network can be given as follows:

An *Artificial Neural Network* is an assembly of an extensive interconnection of fundamental units called *nodes* that are analogous to the *neurons* in the human brain. Further, these *nodes* process a set of *inputs* or *information* and pass on the evaluated *response/output/data* to the adjoining *nodes* in the network.

2.4.2 *Why Artificial Neural Networks?*

In several instances, some of the physics can be neglected to simplify the mathematical formulation of the problem without compromising the validity or even the accuracy of the solution. However, there are several applications where this simplification is not acceptable. Much worse, despite extensive research, several problems cannot be completely formulated due to our limited understanding of the underlying physics. As a result, a precise mathematical modeling of the entire process is extremely challenging in many engineering problems.

In such cases, when the complexity of the problem at hand cannot be solved exactly via existing mathematical models, the principles of artificial neural networks come in handy as they are applicable to problems where a number of parameters influencing the outcome of a system interact in a complex manner. Additionally, as will be discussed in the subsequent sections, it is also possible to include the effect of the parameters that are either unknown or neglected in determining the output of the system using an incomplete set of input parameters.

In the literature, ANN has been employed by researchers to study a variety of problems such as the mechanical [28, 31], electrical [6, 49], and thermophysical properties of the materials [38]. It has also been used to study tribological properties, viz., wear rate and the friction coefficient of fiber composites [57], corrosion studies [40, 47], and surface texture studies [4, 45].

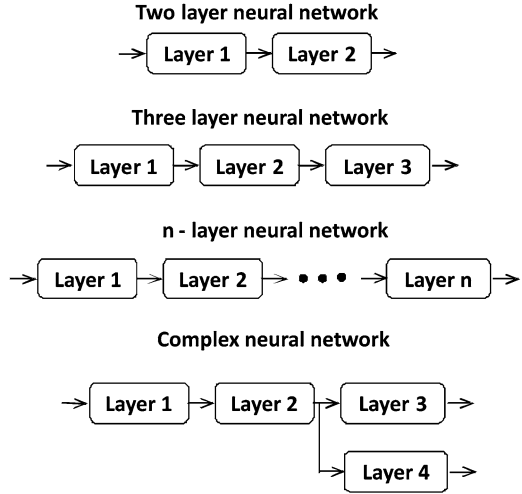
Like the above problems, thermodiffusion is also an equally intricate phenomenon in which despite nearly a century of research, there is still a lack of a single unified theory that can explain the observations at a molecular or microscopic level. One of the main issues is the complexity of the underlying inter-particle and intra-particle interactions, as well as external forces that can affect the liquid at the molecular level. The application of ANN to study thermodiffusion is therefore pertinent.

2.4.3 *Theoretical Formalisms*

In this section, a detailed formalism of an artificial neural network that can be used to study thermodiffusion problems is presented. As mentioned earlier, ANN combines the principles of associative thinking with the precision of mathematical modeling. Development of such a neural network model involves the following steps, each of which will be discussed in detail:

1. Choosing a network topology
2. Database generation
3. Neural network training and testing
4. Neural network validation

Fig. 2.12 Examples of some typical neural network topologies. In each case, the inputs enter the neural network from the left through the first layer. The last layer produces the output of the neural network. Each layer can have one or more nodes



2.4.3.1 Network Topology

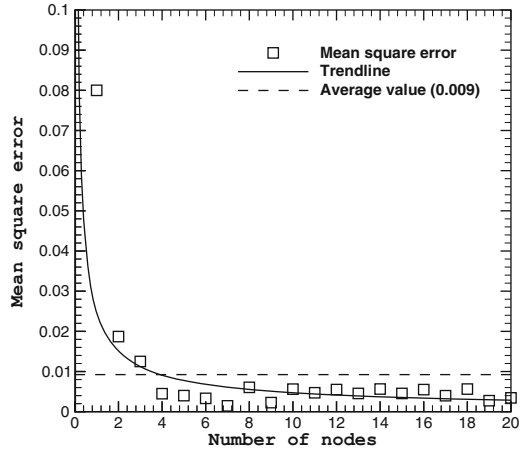
Network topology refers to the structure of the network. Specifically, choosing a network topology involves deciding the number of nodes to be employed in each layer of the neural network, the number of such layers and the way in which the layers are interconnected. Some of the suggested topologies for solving problems related to physics are shown in Fig. 2.12. Any of these topologies can be employed to study thermodiffusion.

As seen in this figure, several complicated topologies are possible. Two points must be noted about these topologies:

1. A layer can have an arbitrary number of nodes, i.e., the number of nodes in each layer can be different. A prior study is essential in determining the number of layers on the neural network as well as the number of nodes to be employed in each layer.
2. Usually, the network connections are such that nodes from each layer is connected to every node in the subsequent layer. All the topologies shown in Fig. 2.12 correspond to a *feed forward neural network*. As the name indicates, the inputs enter the neural network through the first layer on the left and propagate from one layer through the next in one direction (right). The output of the last layer represents the output of the neural network. There are other possible interconnections, but they are out of the current scope. The readers can refer to dedicated works on neural networks that describe the other network implementations in greater depth [24, 27].

To determine a neural network topology that is capable of predicting, say for instance, the Soret coefficient, thermodiffusion coefficient or even the mixture properties such as density and viscosity, the first step is to finalize the number of

Fig. 2.13 The mean square error analysis to determine the number of nodes in an internal layer of the neural network



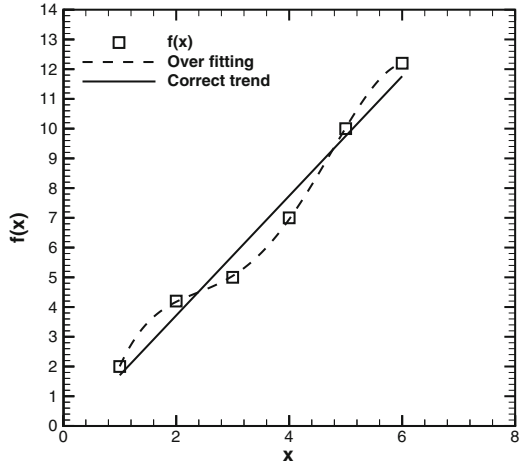
layers in a network. To this end, a three layer network can be employed since it is sufficient to solve most engineering problems. Next, the number of nodes in these layers is determined through the analysis of the neural network. More precisely, the number of nodes are progressively increased until the performance of the neural network stabilizes, i.e., for a given set of input data, the network predictions are compared with the experimental data. The mean square error of all the data are studied by plotting them in a graph as shown in Fig. 2.13. In this example figure, it is evident that increasing the number of nodes beyond 5 does not produce a noticeable improvement in the performance of the neural network. Hence, using five nodes in this layer would suffice.

An appropriate topology is important since the number of network layers and the number of nodes in each layer determine the ability of the network to capture the important thermodiffusion trends in the mixtures. It must be noted that a network with many nodes can result in an over-fitting of the data. On the other hand a network with too few nodes may not be able to predict the thermodiffusion trends accurately. This is illustrated in Fig. 2.14 where the data (with some errors) more or less obey a linear trend. However, with excessive nodes, the error in the data is also modeled by the neural network and it predicts a polynomial behavior of the data.

As mentioned earlier, the input parameters are fed to the neural network through the nodes at the extreme left of the network. Each node processes this information, produces an output, and transfers it to every node in the subsequent layer. In this way, information propagates through the network and the outputs (corresponding to the modeled parameters) are obtained from the last layer of nodes in the network. Mathematically, the output, u , of the i th node in the k th layer of the network is [27]

$$u_i^{(k)} = f^{(k)} \left(b_i^{(k)} + \sum_{j=1}^J u_j^{(k-1)} w_{ji}^{(k)} \right), \quad (2.135)$$

Fig. 2.14 An illustration of the over-fitting of the experimental data by the neural network



where w are *weight coefficients* that scale the inputs to a node and J is the number of nodes in the layer $(k - 1)$. b is called the *bias* term that is included in the above expression to account for the following:

1. Parameters that have been missed in the input parameter set which impact the process and thereby the output variables.
2. Other unknown parameters that might be contributing to the physics of the problem.

In (2.135), f is a *transformation function* that modulates the sum of the bias and weighted inputs. While different types of transformation functions can be employed, two popular functions are

$$f(\zeta) = \tanh(\zeta) = \frac{1 - e^{-2\zeta}}{1 + e^{-2\zeta}}, \quad (2.136a)$$

$$f(\zeta) = \frac{1}{1 + e^{-\zeta}}. \quad (2.136b)$$

2.4.3.2 Database Generation

In this step, experimental data of the quantities of interest, viz., Soret coefficient, thermodiffusion coefficient, thermodiffusion factor, mixture density, mixture viscosity, etc. are collected for various input parameter combinations. In typical thermodiffusion studies, the input parameter set would include the mole fraction of the participating components and pure component properties like the molecular weight, density, and viscosity.

Following the compilation of the database, before using it with an artificial neural network, *standardization* and *normalization* of the database are common practice.

These are necessary and are usually done to shield the neural network from the influence of the absolute value of a particular parameter. Standardization is done by adjusting the input parameters of the database such that each parameter set in the database has a mean of zero and a standard deviation of one. This can be done via the following equation

$$p_{i,:} = \frac{(p'_{i,:} - \bar{p}_i)}{\sigma_i}, \quad (2.137)$$

where $p_{i,:}$ are the values of the i th standardized input parameter, and \bar{p}_i and σ_i are the mean and standard deviations, respectively, of the i th input parameter. $p'_{i,:}$ are the actual values of the parameters in the respective experiments.

Following this, the range of each parameter is normalized such that $p_i \in \{-1, +1\}$. This can be achieved by applying the following transformation to the standardized database.

$$p_{i,:} = \frac{(p_{i,:} - p_{i,:}^{\min})}{(p_{i,:}^{\max} - p_{i,:}^{\min})}, \quad (2.138)$$

where $p_{i,:}^{\min}$ and $p_{i,:}^{\max}$ represent the minimum and maximum values, respectively, of the i th parameter in the standardized database.

2.4.3.3 Neural Network Training

As the input data propagates through each node, it gets transformed via a set of *bias* and *weights* values. The agreement between the output values predicted by the neural network and the experimental data (called the *target* values) is directly governed by the accuracy of the set of weights and bias values. To obtain the optimal combination of the bias and weights values that result in a good network, a search algorithm is applied. This process is called *network training* or simply *training* which will culminate in a network that is capable of predicting the target data with the least error.

For training a neural network, the standardized and normalized database is randomly shuffled and split into two parts. Usually, 60–80% of the randomly shuffled database is employed for training and is called the *training data*. The remaining 40–20% of the unused database is saved to evaluate the trained neural network and is called the *validation data*. These data are not seen by the NN while it is being trained.

For the optimal weight determination problem in hand, one could resort to gradient-based search algorithms or heuristic search methods. The former includes Newton's method, Conjugate gradient method, Levenberg–Marquardt backpropagation (LMBP) algorithm, etc. On the other hand, Genetic algorithm-based searches come in the category of heuristic methods.

A gradient-based training algorithm that is well established in the literature is the *LMBP* algorithm [27] that minimizes a mean square error function over a multidimensional parameter space. This algorithm begins with a network initialization in

which a random set of values for weights and bias are chosen as an initial guess. One could also employ a more systematic initialization method such as the Nguyen and Widrow's algorithm [42]. Following the initialization of the network weights and bias values, the algorithm performs the following steps iteratively:

Step 1: Evaluate the response of the network for the training data set and compare it with the desired experimental data.

Step 2: If the convergence criterion is not reached, update the network weights and bias values, and go to Step 1.

To update the weights, the LMBP algorithm uses an enhanced version of the Newton's method that is derived as follows: In the k th iteration of the algorithm, a Newton's update for a node that receives N input parameters and that are scaled by a weight vector $\mathbf{w} \in \Re^{N \times 1}$, can be written as

$$\mathbf{w}(k+1) = \mathbf{w}(k) - \mathbf{H}_k^{-1} \mathbf{g}_k, \quad (2.139)$$

where the Hessian, \mathbf{H}_k , is a real valued matrix, i.e., $\mathbf{H}_k \in \Re^{N \times N}$ and $\mathbf{g}_k \in \Re^{N \times 1}$ is the gradient of mean square error, E . The subscript, k , in \mathbf{H}_k and \mathbf{g}_k indicates that these quantities are evaluated at $\mathbf{w} = \mathbf{w}(k)$. In other words,

$$\mathbf{H}_k = \nabla^2 E \big|_{\mathbf{w}=\mathbf{w}(k)}, \quad (2.140)$$

$$\mathbf{g}_k = \nabla E \big|_{\mathbf{w}=\mathbf{w}(k)}.$$

In the above equations, E is a measure of the error and is expressed as

$$E = \frac{1}{2\zeta} \sum_{q=1}^{\zeta} (\mathbf{t}_q - \mathbf{y}_q)^T (\mathbf{t}_q - \mathbf{y}_q) = \frac{1}{2\zeta} \sum_{q=1}^{\zeta} \sum_{j=1}^J (t_{q,j} - y_{q,j})^2, \quad (2.141)$$

where ζ is the total number of training vectors that are applied in each iteration. The *target* vector, \mathbf{t} , has J outputs and the vector \mathbf{y} consists of the corresponding output values predicted by the network.

In the expression of the Hessian, the $\nabla^2 E$ term can be written in terms of the Jacobian, \mathbf{J} as

$$\nabla^2 E = \mathbf{J}^T \mathbf{J} + \Phi. \quad (2.142)$$

\mathbf{J} , in the above equation, has the elements

$$\mathbf{J} = \frac{1}{\sqrt{\zeta}} \begin{bmatrix} \frac{\partial(t_1-y_1)}{\partial w_1} & \frac{\partial(t_1-y_1)}{\partial w_2} & \dots & \frac{\partial(t_1-y_1)}{\partial w_N} \\ \frac{\partial(t_2-y_2)}{\partial w_1} & \frac{\partial(t_2-y_2)}{\partial w_2} & \dots & \frac{\partial(t_2-y_2)}{\partial w_N} \\ \vdots & \vdots & \ddots & \vdots \\ \frac{\partial(t_{\zeta J}-y_{\zeta J})}{\partial w_1} & \frac{\partial(t_{\zeta J}-y_{\zeta J})}{\partial w_2} & \dots & \frac{\partial(t_{\zeta J}-y_{\zeta J})}{\partial w_N} \end{bmatrix}. \quad (2.143)$$

Table 2.2 The key steps of the Levenberg–Marquardt backpropagation algorithm [27], reproduced from [52]

Step 1: Initialize network weights and biases.
while $\mathbf{w} \neq \mathbf{w}^*$
for $j = 1, 2, \dots, P$
Step 2: Calculate the network output for a particular data vector.
Step 3: Calculate the j^{th} row of the Jacobian matrix in (2.143).
end for loop
Step 4: Update network weights using (2.149) and check if $\mathbf{w} = \mathbf{w}^*$.
end while loop

Also, Φ in (2.142) is

$$\Phi = \sum_{i=1}^P e_i \nabla^2 e_i, \quad (2.144)$$

where $e_i = (t_i - y_i)/\sqrt{\zeta}$ and $P = \zeta J$. Close to the convergence criterion, \mathbf{w} approaches the optimal value of \mathbf{w}^* , $e_i \rightarrow 0$ and $\Phi \rightarrow 0$. In other words, we can approximate the Hessian as

$$\mathbf{H} \approx \mathbf{J}^T \mathbf{J}. \quad (2.145)$$

Further, the gradient can be written in terms of the Jacobian as

$$\mathbf{g} = \mathbf{J}^T \mathbf{e}, \quad (2.146)$$

and we can rewrite (2.139) as

$$\mathbf{w}(k+1) = \mathbf{w}(k) - [\mathbf{J}_k^T \mathbf{J}_k]^{-1} \mathbf{J}_k^T \mathbf{e}_k. \quad (2.147)$$

Now, it must be noted that in the above equation, the inversion of the Hessian can be an ill-conditioned problem. To overcome this drawback one can introduce a small perturbation to the Hessian and write it as

$$\mathbf{H} \approx \mathbf{J}^T \mathbf{J} + \xi \mathbf{I}, \quad (2.148)$$

where $\mathbf{I} \in \Re^{N \times N}$ is an identity matrix and ξ is a small scalar called the *learning parameter*. Introducing this approximation of Hessian in (2.147), we obtain the Levenberg–Marquardt update as

$$\mathbf{w}(k+1) = \mathbf{w}(k) - [\mathbf{J}_k^T \mathbf{J}_k + \xi_k \mathbf{I}]^{-1} \mathbf{J}_k^T \mathbf{e}_k. \quad (2.149)$$

Theoretically, convergence must be obtained after a large number of iterations. More precisely, as $k \rightarrow \infty$, $\mathbf{e}_k \rightarrow 0$ and $\mathbf{w} \rightarrow \mathbf{w}^*$. In other words, \mathbf{w} converges to the most appropriate weight matrix \mathbf{w}^* that enables the network to predict the target values with minimal error. The key steps of the LMBP algorithm are outlined in Table 2.2.

2.4.3.4 Termination Criterion of the Algorithm

Keeping in mind the numerics of the implementation of the algorithm, the optimal weight determination procedure described above is coupled with a set of termination criterion that are checked at each iteration of the training process. These criteria are as follows:

1. The training is terminated if the mean square error is less than tol_{mse} . The choice of this tolerance value is decided after some numerical experimentation. This is because a very small error tolerance can result in an over-fitting of the experimental data, and with a large value of tol_{mse} there is a risk of developing a neural network model with poor prediction capabilities.
2. During the course of network training, the updated network in each iteration is tested with respect to a small data set. These *test* data are a subset of the training data and are *not* taken from the validation data set. Now, in evaluating these test data, if the network performance does not improve for tol_t successive iterations, then it is assumed that the network training is complete and the training process is terminated.
3. Since the LMBP algorithm is a gradient-based search algorithm, the zero gradient point corresponds to an optimal value. However, an absolute zero gradient is perhaps too stringent a condition to implement. Hence, the training is usually stopped when the gradient in (2.146) is sufficiently small. In other words, the training is terminated if the gradient is less than tol_{grad} .
4. Irrespective of the above conditions for ending the optimization process, the algorithm is terminated if the number of iteration reaches a specified upper limit, i.e., $P \geq P_{\text{max}}$. While the previous three termination criteria indicate some sort of convergence to an optimum, this criterion indicates a poor convergence and must be generally avoided. For this, a large value of P_{max} must be specified. In the thermodiffusion studies, it has been found that the use of $P_{\text{max}} \approx O(10^5)$ is sufficient to ensure that the optimization process terminates in one of the first three conditions, i.e., an optimal set of weights is found.

2.4.3.5 Neural Network Validation

This is the final step in which the generated neural network is tested with some experimental data to ensure that the neural network is well trained. For this step, the part of the database that was not used for the training is generally employed. It is important to ensure that this validation data set is sufficiently diverse. This is to verify the prediction abilities of the neural network for the entire range of the parameters in the input data for which the neural network has been trained.

In addition to the testing of the neural network with respect to the experimental data values, it is also essential to conduct studies on its abilities to predict the important trends. For instance, it should be able to predict the effect of the relative molecular weights in a binary n-alkane mixture, for instance, where we know that

the thermodiffusion process is more pronounced if the relative molecular weights are very large. Also, in some mixtures, a change in the direction of separation has been observed experimentally. A good neural network should be able to predict this direction switch. The application of neural network approach, discussed in this section, to binary liquid mixtures is taken up in detail in Chap. 6. There the ability of the neural network to predict these trends is considered more elaborately.

References

1. Artola PA, Rousseau B, Galliero G (2008) A new model for thermal diffusion: kinetic approach. *J Am Chem Soc* 130:10,963–10,969
2. Blanco P, Bou-Ali M, Platten JK, Urteaga P, Madariaga JA, Santamaria C (2008) Determination of thermal diffusion coefficient in equimolar n-alkane mixtures: empirical correlations. *J Chem Phys* 129:174,504. <http://dx.doi.org/10.1063/1.2945901>
3. Blanco P, Bou-Ali M, Platten JK, de Mezquia DA, Madariaga JA, Santamaria C (2010) Thermodiffusion coefficients of binary and ternary hydrocarbon mixtures. *J Chem Phys* 132:114,506. <http://dx.doi.org/10.1063/1.3354114>
4. Brahme A, Winning M, Raabe D (2009) Prediction of cold rolling texture of steels using an artificial neural network. *Comput Mater Sci* 46(4):800–804. URL <http://www.sciencedirect.com/science/article/pii/S0927025609001839> DOI: 10.1016/j.commatsci.2009.04.014
5. Brenner H (2006) Elementary kinematical model of thermal diffusion in liquids and gases. *Phys Rev E* 74:036,306
6. Cai K, Xia J, Li L, Gui Z (2005) Analysis of the electrical properties of PZT by a BP artificial neural network. *Comput Mater Sci* 34:166–172
7. Debuschewitz C, Köhler W (2001) Molecular origin of thermal diffusion in benzene+cyclohexane mixtures. *Phys Rev Lett* 87:055,901
8. Denbigh KG (1952) The heat of transport in binary regular solutions. *Trans Faraday Soc* 48:1–8
9. Dhont JKG (2004) Therodiffusion of interacting colloids. I. A statistical thermodynamics approach. *J Chem Phys* 120(3):1632–1641
10. Dougherty EL, Drickamer HG (1955a) A theory of thermal diffusion in liquids. *J Chem Phys* 23(5):295
11. Dougherty EL, Drickamer HG (1955b) Thermal diffusion and molecular motion in liquids. *J Phys Chem* 59(5):443–449
12. Eslamian M, Saghir MZ (2009) A dynamic thermodiffusion model for binary liquid mixtures. *Phys Rev E* 80:011,201
13. Eslamian M, Saghir MZ (2009) Microscopic study and modeling of thermodiffusion in binary associating mixtures. *Phys Rev E* 80:061,201
14. Eslamian M, Saghir MZ (2010a) Dynamic thermodiffusion theory for ternary liquid mixtures. *J Non-Equilib Thermodyn* 35:51–73
15. Eslamian M, Saghir MZ (2010b) Investigation of the Soret effect in binary, ternary and quaternary hydrocarbon mixtures: new expressions for thermodiffusion factors in quaternary mixtures. *Int J Therm Sci* 49:2128–2137
16. Eslamian M, Saghir MZ (2011) Estimation of thermodiffusion coefficients in ternary associating mixtures. *Can J Chem Eng* 9999:1–8
17. Eslamian M, Saghir MZ (2011) Non-equilibrium thermodynamic model fro the estimation of soret coefficient in dilute polymer solutions. *Int J Thermophys* 32:652–664
18. Eslamian M, Saghir MZ (2012) Modeling of DNA thermophoresis in dilute solutions using the non-equilibrium thermodynamics approach. *J Non-Equilib Thermodyn* 37:63–76
19. Ghorayeb K, Firoozabadi A (2000) Molecular, pressure, and thermal diffusion in non-ideal multicomponent mixtures. *AIChE J* 46(5):883–891 <http://dx.doi.org/10.1002/aic.690460503>

20. Glasstone S, Laidler KJ, Eyring H (1941) The theory of rate processes. The kinetics of chemical reactions, viscosity, diffusion and electrochemical phenomena. McGraw-Hill, New York
21. de Groot SR, Mazur P (1984) Non-equilibrium thermodynamics. Dover, New York
22. Gross J, Sadowski G (2001) Perturbed-chain saft: an equation of state based on a perturbation theory for chain molecules. *Ind Eng Chem Res* 40(4):1244–1260
23. Gross J, Sadowski G (2002) Modeling polymer systems using the perturbed-chain statistical associating fluid theory equation of state. *Ind Eng Chem Res* 41:1084–1093
24. Gurney K (1997) An introduction to artificial neural networks, 1st edn. UCL, Taylor & Francis Group, 1 Gunpowder Square, Londo EC4A 3DE
25. Guy AG (1986) Prediction of thermal diffusion in binary mixtures of nonelectrolyte liquids by the use of nonequilibrium thermodynamics. *Int J Thermophys* 7:563–572
26. Haase R (1969) Thermodynamics of irreversible processes. Addison-Wesley, Reading
27. Ham FM, Kostanic I (2001) Principles of neurocomputing for science and engineering, 2nd edn. McGraw Hill, New York
28. Hancheng Q, Bocai X, Shangzheng L, Fagen W (2002) Fuzzy neural network modeling of material properties. *J Mater Process Technol* 28:196–200
29. Hartmann S, Königer A, Köhler W (2008) Isotope and isomer effect in thermal diffusion of binary liquid mixtures. In: Köhler W, Wiegand S, Dhont JKG (eds) Thermal nonequilibrium. Proceedings of the eighth international meeting on thermodiffusion. Forschungszentrum Jülich GmbH, Bonn, pp 35–41
30. Hiemenz PC, Lodge TP (2007) Polymer chemistry, 2nd edn. CRC, Boca Raton
31. Hwang RC, Chen YJ, Huang HC (2010) Artificial intelligent analyzer for mechanical properties of rolled steel bar by using neural networks. *Expert Syst Appl* 37(4):3136–3139. URL <http://www.sciencedirect.com/science/article/pii/S0957417409008501> DOI:10.1016/j.eswa.2009.09.069
32. Iacopini S, Piazza R (2003) Thermophoresis in protein Solutions. *Europhys Lett* 63(2):247–253
33. Iacopini S, Rusconi R, Piazza R (2006) The “macromolecular tourist”: universal temperature dependence of thermal diffusion in aqueous colloidal suspensions. *Eur Phys J E* 19:59–67
34. Jhaverl BS, Youngren GK (1988) Three-parameter modification of the Peng-Robinson equation of state to improve volumetric predictions. *SPE Reserv Eng* 3(3):1033–1040
35. Kempers LJTM (1989) A thermodynamic theory of the soret effect in a multicomponent liquid. *J Chem Phys* 90:6541–6548
36. Kempers LJTM (2001) A comprehensive thermodynamic theory of the soret effect in a multicomponent gas, liquid, or solid. *J Chem Phys* 115:6330–6341
37. Khazanovich TN (1967) On theory of thermal diffusion in dilute polymer solutions. *J Polym Sci C: Polym Symp* 16:2463–2468
38. Laugier S, Richon D (2003) Use of artificial neural networks for calculating derived thermodynamic quantities from volumetric property data. *Fluid Phase Equil* 210(2):247–255. URL <http://www.sciencedirect.com/science/article/pii/S0378381203001729> DOI: 10.1016/S0378-3812(03)00172-9
39. Madariaga JA, Santamaria C, Bou-Ali M, Urteaga P, De Mezquia DA (2010) Measurement of thermodiffusion coefficient in n-alkane binary mixtures: composition dependence. *J Phys Chem B* 114:6937–6942. <http://dx.doi.org/10.1021/jp910823c>
40. Martin Ó, De Tiedra P, López M (2010) Artificial neural networks for pitting potential prediction of resistance spot welding joints of AISI 304 austenitic stainless steel. *Corros Sci* 52:2937–2402
41. Morozov KI (2009) Soret effect in molecular mixtures. *Phys Rev E* 79:031,204
42. Nguyen D, Widrow B (1990) Improving the learning speed of 2-layer neural network by choosing initial values of the adaptive weights. *Proc Int Joint Conf Neural Networks* 3:21–26
43. Peng D, Robinson DB (1976) A new two-constant equation of state. *Ind Eng Chem Fundam* 15(1):59–64. <http://dx.doi.org/10.1021/i160057a011>
44. Prigogine I, de Brouckere L, Amand R (1950) Recherches sur la thermodiffusion en phase liquide: (premiere communication). *Physica* 16(7–8):577–598

45. Rashidi A, Hayati M, Rezaei A (2011) Prediction of the relative texture coefficient of nanocrystalline nickel coatings using artificial neural networks. *Solid State Sciences* 13:1589–1593
46. Rauch J, Köhler W (2003) Collective and thermal diffusion in dilute, semidilute, and concentrated solutions of polystyrene in toluene. *J Chem Phys* 119:11,977
47. Rolich T, Rezić I, Ćurković L (2010) Estimation of steel guitar strings corrosion by artificial neural network. *Corros Sci* 52:996–1002
48. Semenov S, Schimpf M (2004) Thermophoresis of dissolved molecules and polymers: consideration of the temperature-induced macroscopic pressure gradient. *Phys Rev E* 69(2):011,201
49. Seo DC, Lee JJ (1999) Damage detection and CFRP laminates using electrical resistance measurement and neural network. *Compos Struct* 47:525–530
50. Shukla K, Firoozabadi A (1998) A new model of thermal diffusion coefficients in binary hydrocarbon mixtures. *Ind Eng Chem Res* 37(8):3331–3342
51. Song S, Peng C (2008) Viscosities of binary and ternary mixtures of water, alcohol, acetone, and hexane. *J Disp Sci Tech* 29(10):1367–1372
52. Srinivasan S, Saghir MZ (2012) Modeling of thermotransport phenomenon in metal alloys using artificial neural networks. *Appl Math Modell*. DOI:10.1016/j.apm.2012.06.018
53. Stadelmaier D, Köhler W (2009) Thermal diffusion of dilute polymer solutions: the role of chain flexibility and the effective segment size. *Macromolecules* 42:9147–9152
54. Tichacek LJ, Kmak WS, Drickamer HG (1956) Thermal diffusion in liquids; the effect of non-ideality and association. *J Phys Chem* 60:660–665
55. Wittko G, Köhler W (2005) Universal isotope effect in thermal diffusion of mixtures containing cyclohexane and cyclohexane-d12. *J Chem Phys* 123:14,506
56. Wittko G, Köhler W (2007) On the temperature dependence of thermal diffusion of liquid mixtures. *Europhys Lett* 78:46,007
57. Zhang Z, Friedrich K, Veiten K (2002) Prediction on tribological properties of short fibre composites using artificial neural networks. *Wear* 252:668–675

Thermodiffusion in Multicomponent Mixtures
Thermodynamic, Algebraic, and Neuro-Computing
Models

Srinivasan, S.; Saghir, M.Z.

2013, XI, 106 p. 41 illus., 5 illus. in color., Softcover

ISBN: 978-1-4614-5598-1